รายงานวิจัยฉบับสมบูรณ์

โครงการ ผลของสารไฟโตเอสโตรเจนต่อการตายของเซลล์แบบอะพอพโทสิสของเซลล์มะเร็งเม็ดเลือดขาว

โดย

รศ.ดร.พญ. รัตนา บรรเจิดพงศ์ชัย
รศ.ดร.ปรัชญา คงทวีเลิศ

ภาควิชาชีวเคมี คณะแพทยศาสตร์ มหาวิทยาลัยเชียงใหม่

พฤศจิกายน 2552

สัญญาเลขที่ RMU5080003

รายงานวิจัยฉบับสมบูรณ์

โครงการ ผลของสารไฟโตเอสโตรเจนต่อการตายของเซลล์แบบอะพอพโทสิส ของเซลล์มะเร็งเม็ดเลือดขาว

โดย

รศ.ดร.พญ. รัตนา บรรเจิดพงศ์ชัย

รศ.ดร.ปรัชญา คงทวีเลิศ

ภาควิชาชีวเคมี คณะแพทยศาสตร์ มหาวิทยาลัยเชียงใหม่

สนับสนุนโดยสำนักงานคณะกรรมการอุดมศึกษา

และสำนักงานกองทุนสนับสนุนการวิจัย

ACKNOWLEDGMENTS

I thank God for His kindness and caring to provide me wisdom to run through this research work. Without His help and grace, this work would be impossible and inefficient.

This work was financially supported by Thailand Research Fund and Commission of Higher Education through out three years.

This work was collaborated with Prof. Dr. Jisnuson Svasti (at Department of Biochemistry, Faculty of Science, Mahidol University and Chulabhorn Research Institute) and Dr. Chantragan Srisomsap at Chulabhorn Research Institute on the part of proteomics. I am grateful to Prof. Dr. Prapon Wilairat who has suggested and given critical comments on the research work. I also would like to thank for Dr. Pantipa Subhasitanont, Dr. Daranee Chokchaichamnankit, Miss Yupa Chanwikrai and Mr. Pathompong Kao-on (research resistant) who helped in the techniques of the proteomics, cytotoxicity assay and Western blotting.

Almost all of this work was performed at Department of Biochemistry and the Medical Science Instrument Center, Faculty of Medicine, Chiang Mai University, where the equipments and instruments were utilized for testing and analyzing the data, the proteomic part was done at Chulabhorn Research Institute in Bangkok, to which I express my sincere gratitude for the facilities by all places.

Finally, I deeply thank my parents, sister and brothers for their prayer support throughout this research project.

Ratana Banjerdpongchai, M.D., Ph.D.
Associate Professor

November 30, 2009

ABSTRACT

Phytoestrogens are very popular as 'alternative' medicine for many kinds of diseases. The apoptotic effects of 9 phytoestrogens, i.e., baicalein (BAI), bisphenol A (BPA), naringenin (NAR), zearalenone (ZEA), puerarin (PUE), daidzein (DAI), genistein (GEN) and biochannin A (BCA) and apigenin (API) on human leukemic HL-60, U937 cells and peripheral blood mononuclear cells were aimed to be studied, including the mechanisms, such as their effects on reactive oxygen species (ROS) production and cell cycle characteristics. Cytotoxicity test was performed using MTT assay and IC_{50} levels of the phytoestrogens were determined. mitochondrial transmembrane potential (MTP) of apoptotic cells was evaluated employing 3, 3'-dihexyloxacarbocyanine iodide and flow cytometry. ROS-producing capacity was measured using 2', 7'-dichlorofluorescein diacetate and flow cytometry. Cell cycle characteristics were studied by propidium iodide staining and flow cytometry. To identify the molecular mechanisms, determination of the caspase-3 and -8 activities was performed using fluorescence-tagged substrates and fluorescence plate reader. The two dimensional gel electrophoresis of cytosolic and membrane proteins was evaluated to compare the protein expression in control and ZEA-treated cells. Immunoblotting of cytochrome c, Bax, Bcl-2 and Bcl-xL was performed. Analysis of cytosolic and mitochondrial calcium ion levels was also performed to evaluate the involvement of mitochondria. Determination calreticulin (ER stress protein) on cell membrane with anti-calreticulin and flow cytometry.

It was found that PBMCs were more resistant to the phytochemicals than both transformed cells. All phytochemicals were cytotoxic to HL-60 and U937 cells in a dose dependent manner, except PUE. All phytochemicals induced apoptosis of U937 and HL-60 cells as evidenced by a decrease in transmitochondrial membrane potential, except PUE. In U937 cells, BAI (20 μg/ml), BPA (20 μg/ml), NAR (50 μg/ml), BCA (10 μg/ml) and ZEA (10 μM), induced ROS generation. In HL-60 cells, NAR (250 μg/ml), ZEA (20 μg/ml) and PUE (50 μg/ml) produced peroxide radicals. In U937 cells, BIS, NAR and ZEA caused cell cycle arrest at G2/M phase and induced DNA fragmentation as evidenced by the presence of subdiploid peak in flow cytometry. Similarly in HL-60 cells, BAI (50 μg/ml), BPA (50 μg/ml), NAR (250 μg/ml), ZEA (50 μg/ml), GEN (50 μg/ml), API (50 μg/ml), and BCA (50 μg/ml) caused G2/M arrest but ZEA at a lower dose (10 μg/ml) produced G0/G1 arrest. Caspase-3 activity was high in a dose-dependent manner in HL-60 cell apoptosis induced by BCA, NAR, BPA and ZEA while stimulated by BAI, BCA, NAR, BPA and ZEA in U937 cell apoptosis.

Zearalenone (ZEA) is a phytoestrogen produced by several *Fusarium* species, such as *F. graminearum*. ZEA had IC_{50} values of cell cytotoxicity using MTT assay in HL-60, U937 and peripheral blood mononuclear cells, as 44, 5.1 and >80 μg/ml, respectively. ZEA-treated human leukemic cells had a typical morphology of apoptotic cells after staining with propidium iodide and examining under fluorescence microscope. ZEA caused a decrease in mitochondrial outer membrane potential in a dose response manner, and cytochrome c release indicating the involvement of mitochondria. Caspase-3 activity increased in a dose-related manner, whereas caspase-8 responsed time dependently. Two dimensional PAGE of U937 cells treated with ZEA showed 3 proteins of difference, i.e., fructose bisphosphate aldolase A, muscle type, lung cancer antigen NY LU 1; glyceraldehydes 3-phosphate dehydrogenase and deoxyuridine triphosphate nucleotidohydrolase, mitochondrial precursor. Proteomics of 24 hour-ZEA-treated HL-60 cells showed 23 membrane proteins of difference including the ER stress proteins, which were 78 kDa glucose-regulated protein (GRP78), heat shock protein 90 and calreticulin. ZEA also induced an enhancement of Ca^{2+} concentration in mitochondria and cytosol. No translocalization of calreticulin, an endoplasmic reticulum (ER) protein, from ER to the cell membrane at 1 h of ZEA treatment. Bax was upregulated time-dependently and there was downregulation of Bcl-xL expression in immunoblotting. PI3-K inhibitor (wortmannin) and MEK inhibitor (PD98059) showed synergistic effect on ZEA-induced apoptosis. Vinblastine (a chemotherapeutic drug) also enhanced ZEA-mediated cell apoptosis by the reduction of MTP.

Taken together, 9 phytoestrogens could induced human human leukemic cell apoptosis via mitochondria and caspase-3. Moreover, the molecular mechanism of ZEA-inhuced human leukemic apoptotic cell death involved caspase-8 activity, ER stress pathway, thus, demonstrating the involvement of the intrinsic (mitochondria), extrinsic and ER stress pathways in apoptotic cell death.

Keywords: HL-60 cell, U937 cell, phytoestrogen, apoptosis, zearalenone, mitochondrial pathway, ER stress

บทคัดย่อ

สารไฟโตเอสโตรเจนเป็นที่นิยมในการรักษาแพทย์ทางเลือกสำหรับโรคหลายชนิด วัตถุประสงค์ของโครงการคือ ศึกษาผลการตายแบบอะพอพทิสของสารไฟโตเอสโตรเจน 9 ชนิด ได้แก่ ไบคาเลน, บิสฟีนอล เอ, นารินเจนนิน, ซีราลีโนน, เพอรารีน, ไดอิดเซอิน, เจนนิสทีน, ไบโอแชนนิน เอ และ เอพิเจนนิน ต่อเซลล์มะเร็งเม็ดเลือดขาวมนุษย์ HL-60 และ U937 และเซลล์เม็ดเลือดขาวปกติ รวมทั้งกลไกการทำให้ตาย ได้แก่ ผลของสารไฟโตเอสโตรเจนต่อการผลิตสารอนุมูลอิสระ และลักษณะวัฏจักรเซลล์ การทดสอบความเป็นพิษต่อเซลล์ใช้การวัดด้วย MTT หาค่าความเข้มข้นของสารไฟโตเอสโตรเจนที่เป็นพิษต่อเซลล์ร้อยละ 50 (IC_{50}) และวัดค่าความต่างศักย์ไฟฟ้าของอะพอพโทติกเซลล์โดยใช้สาร 3, 3'-dihexyloxacarbocyanine iodide ด้วยเทคนิคโฟลไซโตมิเตอร์ การวัดความสามารถในการผลิตสารอนุมูลอิสระโดยใช้ 2', 7'-dichlorofluorescein diacetate ด้วยเทคนิคโฟลไซโตมิเตอร์ ศึกษาลักษณะวัฏจักรเซลล์โดยย้อมเซลล์ด้วยโพรพิเดียมไอโอไดด์และเทคนิคโฟลไซโตเมทรี ศึกษากลไกในระดับโมเลกุลโดยวัดการทำงานของเอนไซม์คาสเพส-3 และ -8 โดยใช้สับสตรทที่ติดด้วยสารเรืองแสง เปรียบเทียบการแสดงออกของโปรตีนโดยเทคนิคโปรตีโอมิคส์ของเซลล์กลุ่มควบคุมและเซลล์ที่ให้สารซีราลีโนน ทำอิมมูโนบล็อทของโปรตีน cytochrome c, Bax, Bcl-2 และ Bcl-xL วัดระดับแคลเซียมในไมโตคอนเดรียและไซโตซอลเพื่อดูความสัมพันธ์ของไมโตคอนเดรียด้วย ตรวจการแสดงออกของโปรตีนที่เกี่ยวข้องกับภาวะเครียดอีอาร์ที่ผิวเซลล์ด้วยแอนติบอดี้ต่อแคลเรติคูลิน

ผลการทดลองพบว่า เซลล์ PBMCs ต้านต่อการกระตุ้นให้ตายจากสารไฟโตเอสโตรเจนมากกว่าเซลล์มะเร็ง สารไฟโตเอสโตรเจนทั้งหมดทำให้เซลล์มะเร็งเม็ดเลือดขาวมนุษย์ HL-60 และ U937 ตายยกเว้นสารเพอรารีน สารไฟโตเอสโตรเจนทั้งหมดทำให้ศักย์ไฟฟ้าของไมโตคอนเดรียลเมมเบรนลดลงในเซลล์ U937 และ HL-60 ยกเว้นเพอรารีน ในเซลล์ U937 ไบคาเลน (20 ไมโครกรัม/มิลลิลิตร) บิสฟีนอลเอ (20 ไมโครกรัม/มิลลิลิตร) นารินเจนนิน (50 ไมโครกรัม/มิลลิลิตร) ไบโอแชนนิน (10 ไมโครกรัม/มิลลิลิตร) และซีราลีโนน (10 ไมโครกรัม/มิลลิลิตร) ก่อให้เกิดสารอนุมูลอิสระ ส่วนในเซลล์ HL-60 สารนารินเจนนิน (250 ไมโครกรัม/มิลลิลิตร) ซีราลีโนน (20 ไมโครกรัม/มิลลิลิตร) และเพอรารีน (50 ไมโครกรัม/มิลลิลิตร) ผลิตสารอนุมูลอิสระเปอร์ออกไซด์ ในเซลล์ U937 บิสฟีนอล นารินเจนนิน และ ซีราลีโนนทำให้วัฏจักรหยุดที่เฟส G2/M และก่อให้เกิดการแตกหักของดีเอ็นเอโดยการปรากฏของ subdiploid peak ในเทคนิคโฟลไซโตเมทรีในทำนองเดียวกัน ในเซลล์ HL-60 ไบคาเลน (50 ไมโครกรัม/มิลลิลิตร) บิสฟีนอลเอ (50 ไมโครกรัม/มิลลิลิตร) นารินเจนนิน (250 ไมโครกรัม/มิลลิลิตร) ซีราลีโนน (50 ไมโครกรัม/ลิตร) เจนนิสทีน (50 ไมโครกรัม/มิลลิลิตร) เอพิเจนนิน (50 ไมโครกรัม/มิลลิลิตร) และ ไบโอแชนนินเอ(50 ไมโครกรัม/มิลลิลิตร) ทำให้หยุดที่ G2M แต่ซีราลีโนนที่ความเข้มข้นต่ำกว่า (10 ไมโครกรัม/

มิลลิลิตร) ทำให้วัฏจักรเซลล์หยุดที่ G0/G1 การทำงานของเอนไซม์คาสเพส-3 สูงขึ้นเมื่อความเข้มข้นของไฟโตเอสโตรเจนเพิ่มขึ้นในเซลล์ HL-60 เมื่อกระตุ้นด้วย ไบคาเลน นารินเจนนิน บิสฟีนอลเอ และ ซีราลีโนน ส่วนในการตายอะพอพโทสิสของเซลล์ U937 เอนไซม์คาสเพส-3 เพิ่มขึ้นเป็นไปตาม dose response เมื่อกระตุ้นด้วย ไบคาเลน ไบโอแชนนินเอ นารินเจนนิน บิสฟีนอลเอ และซีราลีโนน

ซีราลีโนนเป็นไฟโตเอสโตรเจนที่สร้างจากเชื้อราในสายพันธุ์ *Fusarium* เช่น *F. graminearum* ค่าเปอร์เซ็นต์การตายที่ 50 ของซีราลีโนนในการทดสอบความเป็นพิษต่อเซลล์ HL-60, U937 และเซลล์เม็ดเลือดขาวปกติเท่ากับ 44, 5.1 และมากกว่า 80 ไมโครกรัม/มิลลิลิตร ตามลำดับ เซลล์มะเร็งเม็ดเลือดขาวเมื่อได้รับสารไฟโตเอสโตรเจนซีราลีโนนจะมีรูปร่างเซลล์เข้าได้กับอะพอพโทติกเซลล์หลังจากย้อมด้วยโพรพิเดียมไอโอไดด์ และดูด้วยกล้องฟลูโอเรสเซนส์ ซีราลีโนนทำให้ศักย์ไฟฟ้าของไมโตคอนเดรียลเมมเบรนลดลงตาม dose response และก่อให้เกิดการหลั่ง cytochrome c ไปที่ไซโตซอล แสดงถึงความสัมพันธ์กับไมโตคอนเดรีย การทำงานของเอนไซม์คาสเพส-3 เพิ่มขึ้นเป็น dose response ขณะที่การทำงานของคาสเพส-8 เป็นแบบ time dependent จากการศึกษาโพลีอะคริลาไมด์เจลอิเลคโตรโฟรีสิสแบบ 2 มิติหรือโปรตีโอมิคส์ เซลล์ U937 ที่ได้รับซีราลีโนนมีโปรตีนที่แตกต่างกัน 3 ชนิด คือ fructose bisphosphate aldolase A, muscle type, lung cancer antigen NY LU 1; glyeraldehyde 3-phosphate dehydrogenase และ deoxyuridine triphosphate nucleotidohydrolase, mitochondrial precursor ส่วนโปรตีโอมิคส์ของเซลล์ HL-60 เมื่อให้ซีราลีโนนนาน 24 ชั่วโมง แสดงโปรตีนที่มีการแสดงออกแตกต่างกัน 23 ชนิด ได้แก่ โปรตีนในภาวะเครียดอีอาร์ คือ 78 kDa glucose-regulated protein (GRP78), heat shock protein 90 และ แคลเรติคูลิน ซีราลีโนนกระตุ้นการเพิ่มขึ้นของแคลเซียมไอออนในไมโตคอนเดรียและไซโตซอล ไม่มีการเคลื่อนย้ายของแคลเรติคูลิน (โปรตีนของภาวะเครียดอีอาร์) จากอีอาร์ไปที่เซลล์เมมเบรนที่ 1 ชั่วโมงของการให้สารซีราลีโนน การแสดงออกของโปรตีน Bax เพิ่มขึ้นตามเวลา และการแสดงออกของ Bcl-xL ลดลงเมื่อเมื่อทำอิมมูโนบล็อต สาร wortmannin และ MEK inhibitor (PD98059) มีฤทธิ์เสริมกับซีราลีโนนในการกระตุ้นเซลล์มะเร็งมนุษย์ให้ตายแบบอะพอพโทสิส ยาเคมีบำบัดวินบลาสตินมีฤทธิ์เสริมในการทำให้เซลล์มะเร็งเม็ดเลือดขาวตายแบบอะพอพโทสิสโดยไปลดศักย์ไฟฟ้าของไมโตคอนเดรียลเมมเบรน

โดยสรุป ไฟโตเอสโตรเจนทั้ง 9 ตัวสามารถทำให้เซลล์มะเร็งเม็ดเลือดขาวตายแบบอะพอพโทสิสโดยไปลดศักย์ไฟฟ้าของไมโตคอนเดรียลเมมเบรน และคาสเพส-3 นอกจากนี้ กลไกในระดับโมเลกุลของการตายแบบอะพอพโทสิสในเซลล์มะเร็งเม็ดเลือดขาวเมื่อกระตุ้นด้วยซีราลีโนนสัมพันธ์กับการทำงานของคาสเพส-8 ภาวะเครียดอีอาร์ ดังนั้น แสดงว่า วิถีการตายเกี่ยวข้องกับวิถีภายใน (ไมโตคอนเดรีย) วิถีภายนอกและภาวะเครียดอีอาร์

คำสำคัญ: เซลล์ HL-60 cell, เซลล์ U937, สารไฟโตเอสโตรเจน, การตายอะพอพโทสิส, ซีราลีโนน, วิถีไมโตคอนเดรีย, ภาวะเครียดอีอาร์

ABBREVIATIONS

AIF	apoptosis inducing factor
Apaf-1	apoptotic protease activating factor-1
API	apigenin
b.w.	body weight
BAI	baicalein
BCA	biochannin A
BPA	bisphenol A
CRT	calreticulin
2-D	two dimension
dATP	deoxyadenosine triphosphate
Ca^{2+}	calcium ion
CO_2	carbon dioxide
CRT	calreticulin
DAI	daidzein
DEVD-AMC	N-acetyl-Asp-Glu-Val-Asp-AMC (7-amino-4-methylcoumarin)
$DiOC_6$	3,3'-dihexyloxacarbocyanine iodide
DMSO	dimethyl sulfoxide
DNA	deoxyribonucleic acid
DTT	dithiothreitol
ER	endoplasmic reticulum
ERp	endoplasmic reticulum protein
FACScan	fluorescence-activating cell scanning
FBS	fetal bovine serum
FITC	fluorescein isothiocyanate
Fluo3-AM	Fluo-3 acetoxymethyl ester
GAPDH	glyceraldehyde 3-phosphate dehydrogenase
GEN	genistein
GRP78	78 kDa glucose regulated protein
h	hour
HL-60	human promyelocytic leukemic cells
H_2O_2	hydrogen peroxide
IC_{50}	inhibition concentration at 50%
IgG	immunoglobulin G
IETD-AMC	N-acetyl-Ile-Glu-Thr-Asp-AMC (7-amino-4-methylcoumarin)
Kg	kilogram
μg	microgram
min	minute
ml	milliliter
mg	milligram
mm	millimeter
mM	millimolar
NAR	naringenin
ng	nanogram
nm	nanometer
MTP	mitochondrial transmembrane potential
MTT	3-(4,5-dimethyl)-2,5-diphenyl tetrazolium bromide
PAGE	polyacrylamide gel electrophoresis
PBS	phosphate buffered-saline

PBMCs	peripheral blood mononuclear cells
PUE	puerarin
Rhod2-AM	Rhod-2 acetoxymethyl ester
ROS	reactive oxygen species
SDS	sodium dodecyl sulfate
U937	human monocytic leukemic cells
V	volt
ZEA	zearalenone

TABLE LISTS **Pages**

FIGURE LISTS **Pages**

CONTENTS **Pages**

INTRODUCTION

Xenoestrogens and phytoestrogens

Plant extracts containing phytohormones are very popular as alternative medicine for many kinds of diseases. They are especially favored by women who enter menopause an concerned about the side effects of hormone replacement therapy. However, adverse health effects of phytoestrogens have often been ignored. Baicalein, bisphenol A, naringenin, zearalenone, biochanin A, genistein and daidsein, puerarin, and apigenin were reported for their biological activities as follows.

Baicalein

Baicalein (BAI) is a flavonoid extracted from the root of *Scutellaria baicalensis* Georgi, a medicinal plant traditionally used in Oriental medicine. BAI exerts either proapoptotic or anti-apoptotic effects in different cell types. BAI induces heme oxygenase-1 (HO-1) gene expression at both the mRNA and protein levels, and the BAI-induced HO-1 protein is blocked by adding cycloheximide or actinomycin D. Activation of ERK, but not JNK or p38, proteins via induction of phosphorylation in accordance with increasing intracellular peroxide levels is detected in BAI-treated RAW264.7 macrophages. The addition of ERK inhibitor, PD98059, (but not the p38 inhibitor, SB203580, or the JNK inhibitor, SP600125) and the chemical antioxidant, N-acetyl cysteine (NAC) significantly reduce BAI-induced HO-1 protein expression by respectively blocking ERK protein phosphorylation and intracellular peroxide production. Additionally, BAI effectively protects RAW264.7 cells from hydrogen peroxide (H_2O_2)-induced cytotoxicity, and the preventive effect is attenuated by the addition of HO inhibitor, SnPP, and the ERK inhibitor, PD98059. H_2O_2-induced apoptotic events including hypodiploid cells, DNA fragmentation, activation of caspase-3 enzyme activity, and a loss in the mitochondrial membrane potential with the concomitant release of cytochrome c from mitochondrial membrane to cytosol are suppressed by the addition of BAI. Blocking HO-1 protein expression by the HO-1 antisense oligonucleotide attenuates the protective effect of BAI against H_2O_2-induced apoptosis by suppressing HO-1 gene expression in macrophages. Overpression of the HO-1 protein inhibits H_2O_2-induced apoptotic events such as DNA fragmentation and hypodiploid cells by reducing intracellular peroxide production induced by H_2O_2, compared with those events in neo-control (neo-RAW264.7) cells., In addition, CO, but not bilirubin and biliverdin, addition inhibits H_2O_2-induced cytotoxicity in macrophages. It suggests that CO can be responsible for the protective effect associated with HO-1 expression. HO-1 gene expression is induced through a ROS-dependent manner suppressing H_2O_2-induced apoptotic cell death (1).

Human gastric cancer AGS cells were separately treated with 12-hydroxyeicosatetraenoic acid (12-HETE, a metabolite of 12-LOX) and baicalein. MTT assay revealed that the absorbance of the 12-HETE-treated group is significantly ($p<0.01$) higher than that of control group and the absorbance of baicalein-treated is significantly ($p<0.01$) less than that of control group, and that 48 h after treatment the apoptosis index of baicalein-treated group is significantly ($p<0.01$) higher than that of untreated group and is significantly ($p<0.01$) lower in the 12-HETE-treated group. Western blotting analysis is used to investigate the mechanism of these effects. The concentration of phosphorylated ERK1/2 in cells treated with 40 nM baicalein is significantly ($p<0.05$) lower than in the untreated group. The expression level of bcl-2 is up-regulated and down-regulated after separate treatment with 12-HETE and baicalein, respectively, and both of these effects could be blocked by PD98059.

Protein kinase C (PKC) activity is increased by treatment with 12-HETE and reduced by treatment with baicalein ($p<0.05$). The PKC inhibitor BIM (bisindolymaleimide-I) blocks the phosporylation of ERK1/2 and activation of PKC induced by 12-LOX. When pretreated with BIM, the concentration of phosphor-ERK1/2 or bcl-2 in BIM + 12-HETE-treated group is significantly ($p<0.05$) lower than in the treated with 12-HETE only, and the concentration in the BIM + baicalein treated group is significantly ($p<0.05$) higher that treated with baicalein only. Via the metabolites, 12-LOX abolishs proliferation of AGS cells and protect cells from apoptosis by activating the ERK1/2 pathway, and eventually, enhances expression of bcl-2. PKC is also involved in the activation of ERK1/2 induced by 12-LOX, 12-LOX inhibitors would be potentially powerful anticancer agents for prevention and cure of human gastric cancer (2).

BAI prevents loss of human glioma cell viability and apoptosis induced by cisplatin in a dose-dependent fashion over the concentrations of 2-10 μM. Exposure of cells to baicalein without cisplatin did not affect cell viability. Western blot analysis demonstrates that cisplatin induces activation of ERK, which is not affected by BAI. BAI prevents Bax expression, mitochondrial depolarization, cytochrome c release from mitochondria, and caspase activation induced by cisplatin. BAI prevents cisplatin-induced apoptosis through inhibition of the mitochondrial depolarization in human glioma cells (3).

Bisphenol A

Xenoestrogens or Environmental estrogens are compounds other than physiological estrogens that can nonetheless evoke estrogenic responses. Deldrin, endosulfan and the DDT metabolite o,*p*'-dichlorodiphenylethylene (DDE) are organochlorine pesticides. Detergents used in plastics manufacturing (e.g. *p*-nonylphenol) and a common precursor monomer that leaches from polycarbonate plastics (bisphenol A; BPA) are widespread contaminants in food and water via packaging, and as manufacturing byproducts in the environment (4). Naturally occurring estrogens from plants and molds can also be abundant; phytoestrogens coumestrol, which is present in alfalfa sprouts and red clover (entering the food cycle via animals grazing in pastures containing this plant (5). Some estrogen mimetics (such as diethylstilbesterol, DES) were designed as pharmaceuticals, but later found to have health-threatening side effects such as vaginal cancer in the neonatally exposed (6). Both estradiol (E2) and compounds representing various classes of xenoestrogens (DES, coumestrol, BPA, DDE, nonylphenol, endosulfan and dieldrin) act via a membrane version of the estrogen receptor-alpha on pituitary cells, and can provoke calcium ion influx via L-type channels, leading to prolactin secretion (7).

Bisphenol A (BPA; CAS No. 80-05-7) is a monomer component of polycarbonate plastics and epoxy resins. These resins are used in numerous consumer products, including food-contact plastics. Over the past decade, a number of reports have implicated that BPA as a potential endocrine disrupting chemicals (EDCs), based primarily on the results of in vitro studies that have been equivocally confirmed in vivo. All the available data, assessed using the weight-of-evidence approach recommended by International Agency for Research on Cancer (IARC) and U.S. Environmental Protection Agency (EPA), indicating that BPA is not likely to be carcinogenic to humans. The results of short-term tests of genetic toxicity demonstrate that BPA is without genotoxic or mutagenic activity in vivo. The metabolic data which do not support that formation of potentially reactive intermediates and, moreover, which demonstrate that BPA is rapidly glucuronidated and excreted (8).

BPA induces reactive oxygen species and apoptosis in mesencephalic neuronal cells (9). BPA caused apoptosis in cultured rat Sertoli cells (10) and central neural cells during early development of *Xenopus laevis* (11). BPA induces apoptosis and G2-to-M arrest of ovarian granulose cells (12). BPA increases the expression of Bax and concomitantly decreases the expression of Bcl-2 at both protein and mRNA levels of granulose cells. Whereas BPA up-regulates PCNA and bcl-2 mRNA expression and down-regulate the bax mRNA expression in ovarian cancer PEO4 cells (13). N-4-noniphenol and BPA can inhibit apoptosis induced by estrogen deletion in breast cancer T47D cells (14).

In cultured rat hippocampal neurons, 17beta-estradiol (E2) and BPA significantly inhibits the staurosporine-induced release of lactate dehydrogenase. In cortical neurons, BPA significantly inhibits the LDH release, while E2 does not. In hippocampal neurons, E2 and BPA significantly inhibit the staurosporine-induced increase in caspase-3 activity. In cortical neurons, BPA and 4-nonylphenol (NP) significantly inhibits the increase in caspase-3 activity, while E2 does not. BPA and 4-nonylphenol might impede normal brain development by inhibiting desirable neuronal cell apoptosis, interfering with caspase-3 activation (15).

BPA is not able to induce the proliferation in human breast cancer MCF-7 cells, but turns out to be a very potent inhibitor of apoptosis. BPA does not act in a classical estrogen like manner in MCF-7 breast cancer cell line (16).

BPA mobilizes intracellular calcium ion in intact TM4 Sertoli cell line in a manner consistant with the inhibition of ER calcium ion pumps. BPA decreases the viability of TM4 cell, and effect that is reversed by either a caspase inhibitor or by BAPTA (which chelates free intracellular calcium ions), and is therefore consistent with calcium dependent cell death via apoptosis (17).

BPA and hydroquinone (HQ) are present in dental resin materials. BPA produces no detectable amount of ESR signal. The acceleration of hydroquinone by BPA results in the production of SQ. (semiquinone radical). The BPA-enhanced SQ. production may occur through either SQ. regeneration by electron transfer from BPA working as an antioxidant or the O2-scavenging activity of BPA. SQ. intensity of HQ/BPA is reduced by lower concentrations of ascorbate, epigallocatechin, gallate and quercetin, but significantly enhanced by gallic acid. At higher concentrations, they act as prooxidant, suggesting their bimodal actions (18).

Naringenin

Naringenin (NAR), a flavonoid, has shown cytotoxicity in various human cancer cell lines and inhibitory effect son tumor growth. Exposure of HL-60 cells to NAR induces apoptosis dose-dependently up until 0.5 mM, but not at 1 mM as demonstrated by a quantitative analysis of nuclear morphological change and flow cytometirc analysis. An extensive inhibitor for caspases, abolishes the NAR-induced apoptosis. The apoptosis-triggering concentration of NAR is shown to promote the activation of caspase-3, and slightly promote that of caspase-9, but had no effect on caspase-8. NAR-induced apoptosis caused by induction of specific NF-kappaB-binding activity and involving the degradation of IkappaBalpha. Incubation with a high concentration of NAR (1 mM) redues intracellular ATP levels, but no change is observed at lower concentrations. NAR increases dose-dependently hyperpolarization of mitochondrial membrane potential. The result indicates a common pathway to apoptosis and necrosis by NAR. The mechanism involves the activation of NF-kappaB and correlates with degradation of IkappaBalpha. Induction of necrosis by NAR suggests causing by intracellular ATP depletion and mitochondrial dysfunction (19).

NAR has anti-proliferative effects in many cancer cell lines. Antioxidant activities, kinase and glucose uptake inhibition have been proposed as molecular mechanisms for these effects. In addition, an anti-estrogenic activity has been observed but the mechanism is not known. Cancer cells containing transfected (human cervix epitheloid carcinoma HeLa cells) or endogenous estrogen receptor (ER) alpha (human hepatoma HepG2 cells) or ERbeta (human colon adenocarcinoma DLD-1 cells) are studied. NAR exerts an anti-proliferative effect only in the presence of ERalphaa or ERbeta. NAR stimulation induces the activation of p38/MAPK leading to the pro-apoptotic caspase-3 activation and to the poly(ADP-ribose) polymerase cleavage in all cancer cell lines considered. NAR shows an anti-estrogenic effect only in ERalpha containing cells; whereas in ERbeta containing cells, NAR mimics the 17beta-estradiol effects (20).

Zearalenone

Zearalenone (ZEA) is a resorcyclic acid lactone, chemically described as 6-[10-hydroxy-oxo-trans-1-undecenyl]-B-resorcyclic acid lactone. Food, snacks, dried fruits, dried vegetables and beaverages such as beer, are found contaminated with ZEA (21, 22).

Considering the mean levels of ZEA in the principal foods and their consumption, the average daily intakes of ZEA ranged among adults from 0.8-29 ng/kg b.w., while small children have the highest average daily intakes ranging from 6-55 ng/kg b.w./day (23).

Zearalenone and its metabolites (5-hydroxy-2,4-deoxy-zearalenone; zeralenol) are non-steroidal estrogenic mycotoxins produced as secondary metabolites by fungi of the genus *Fusarium*. As this fungi grow on grains such as corn and wheat, the main uptake occurs through ingestion of cereals which have fungal decay (24-26). ZEA is one of the strongest naturally occurring estrogenic compounds.

An incubation of bovine lymphocytes with 0.1-2 µM ZEA significantly increases the number of sister chromatid exchanges and chromosomal aberration (27). At concentrations of 5-20 µM ZEA induced micronuclei in Vero Monkey kidney cells (28). This is partially prevented by the addition of 25 µM vitamin E. This was confirmed by another study, in which ZEA also formed DNA adducts in mouse liver and kidney after a single i.p. dosage of 2 mg/kg (29).

No evidence for apoptosis by FACS-analysis for a hypodiploid DNA peak was found after incubation of bovine lymphocytes with 0.1-2 µM ZEA (27), but it was demonstrated that apoptosis occurs in Vero, Caco-2 and DOK cells at concentrations of 10-40 µM ZEA by DNA ladder formation and observations of apoptotic bodies (30). Moreover, ZEA induces cell cycle arrest in the three cell-lines characterized by an increase of the number of cells in G2/M phase (30). ZEA induced apoptosis in rat sperm cells after a single i.p dose of 5 mg/kg which was shown by TUNEL labeling and DNA ladder formation (31). ZEA target mitochondria and /or lysosomes, induces lipid peroxidation, cell death and inhibits protein and DNA syntheses (32). It has been reported that ZEA shows less cytotoxicity to mammalian cells cultures in the in vitro models tested (C5-O, Caco-2, V79 and CHO-K1 cell lines (33).

The effect of ZEA on freshly isolated human peripheral blood mononuclear cells (PBMC) in relation to proliferation and cell death patterns of untreated and mitogen-activated cells was demonstrated (34). The higher concentration of 30 mg/ml ZEA was found to totally inhibit T and B lymphocyte proliferation from the stimulation with phytohemagglutinin and pokeweed mitogen. The inhibitory effects of ZEA were further related to cell necrosis/apoptosis. Flow cytometry analysis shows a distinct necrotic effect on PBMC, irrespective of mitogen stimulation, whereas apoptotic activity was less evident. Necrosis was observed in both the lymphocyte and monocyte/granulocyte gates. Measurement of ZEA-induced intracellular Ca^{2+} mobilization shows an increase of both Ca^{2+} levels and the number of cells with high Ca^{2+} only in the monocyte/granulocyte gated cells. Using phenylmethyl sulfonyl fluoride (PMSF), a serine protease inhibitor, and ammonium chloride, a lysosomal inhibitor, both associates with cell necrosis inhibition, it is shown that PMSF at 0.05 mM and NH(4)Cl at 1 and 10 mM reduce the cytopathic effects induced by 30 μg/ml ZEA, whereas apoptosis was less affected. Expose of PBMC to 1 μg/ml ZEA did not alter the viability of the cells (34).

ZEA can stimulate proliferation of MCF-7 cells with inducing a profound increase in S phase and a modest increase in G(2)M phase that is accompanied by a decrease in G(0)G(1) phase. ZEA can inhibit apoptosis in MCF-7 cells following estrogen ablation at a range of concentration of 2 - 96 nM. Western blot and RT-PCR analysis reveals the anti-apoptotic bcl-2 is upregulated at both protein and mRNA level, together with the downregulation of pro-apoptotic bax. ZEA has possessed comparative estrogenic activity and could promote the progression of MCF-7 cells through the cell cycle by a decreasing in the G(0)G(1) phase and by a significant increase in S phase. The proliferation activity of ZEA is due to inhibition of apoptosis through regulation of bax/bcl-2 expression (Yu et al. 2005;Yu, Zhang, & Wu 2005). ZEA functions as an antiapoptotic agent by increasing the survival of MCF-7 cell cultures undergoing apoptosis caused by serum withdrawal. Treatment of these cells with 100 nM ZEA induced cell cycle transit after increases in the expression of c-myc mRNA and cyclin D1, A and B1 and downregulation of p27(Kip-1). G(1)/G(2)-phase kinase activity and phosphorylation of the retinoblastoma gene product was also evident. Flow cytometric analysis demonstrates entry of cells into S and G(2)M phases of the cell cycle, and phosphorylation of histone H3 occurs 36 h after ZEA treatment. Ectopic expression of a dominant-negative p21 (ras) completely abolishes the ZEA-induced DNA synthesis in these cells, and the specific inhibitor PD98059 for mitogen/extracellular-regulated protein kinase kinase arrests S-phase entry induced by ZEA (35).

Biochanin A, Genistein and Daidsein

Isoflavones inhibit or prevent a wide variety of chronic diseases and depress the growth of some types of tumor cells, e.g., prostate adenomacarcinoma. Genistein (5,7,4'-trihydroxyisoflavone; GEN) is the major isoflavone in soy. Biochanin A (BCA), and daidsein (DAI) are also polyphenols from soy.

Polyphenols exhibit different abilities to modulate IGF-1-nduced proliferation, cell cycle progression (flow cytometry) and apoptosis (Annexin V/propidium iodide and terminal deoxynucleotidyltransferase-mediated deoxyuridine 5'-triphosphate nick end labeling. GEN and BCA exhibit dose-dependent inhibition of growth with 50% inhibitory concentration (IC50) between 25 and 40 μM, whereas DAI is less potent with IC0 of >60 μM. GEN potently induces G2M cell cycle arrest. GEN and BCA, but not DAI, counteracts the antiapoptotic effects of IGF-I. Human prostate epithelial cells grown in growth factor-supplemented medium are also sensitive to growth inhibition by polyphenols. GEN and BCA reduce the insulin receptor substrate-1 (IRS-1) content of AT6.3 cells and prevent the down-regulation of IGF-I receptor beta in response to IGF-I binding. IGF-1 stimulated proliferation is dependent on activation of mitogen-activated protein kinase/extracellular signal-regulated-kinase (ERK) and phosphatidylinositide 3-kinase pathways. Several polyphenols suppress phosphorylation of AKT and ERK1/2, and more potently inhibit IRS-1 tyrosyl phosphorylation after IGF-I exposure (36). BCA induces a dose-dependent inhibition of proliferation and [(3)H]thymidine incorporation that correlated with increased DNA fragmentation, indicative of apoptosis. Western blot analyses of cell cycle regulatory proteins revealed that BCA significantly decreased expression of cyclin B and p21, whereas flow cytometry showed that cells were accumulated in the G0G1 phase. In mice with LNCaP xenografts, BCA significantly reduces tumor size and incidence (37).

GEN, BCA and DAI inhibit growth of human hepatoma cell lines (HepG2, Hep3B, Huh7, PCL, and HA22T) in a dose-dependent manner. DNA fragmentation studies and the TUNEL assay demonstrated that these isoflavones caused tumor cell death by induction of apoptosis. Activation of caspase-3 and cleavage of the caspase-3 substrate, poly(ADP-ribose)polymerase, is seen in hepatoma cells after 24 hours' exposure to isoflavones. In addition, isoflavone cytotoxicity correlates with downregualtion of Bcl-2 and Bcl-xL expression. Synergistic effects of the three isoflavones are observed on cell growth inhibition, apoptosis induction, and anti-apoptotic protein expression. Flow cytometry shows that GEN, but not BCA and DAI, induces progressive and sustained accumulation of hepatoma cancer cells in the G2M phase as a result of arrest, but not apoptosis, showing that cell cycle arrest is not necessary for apoptosis. Furthermore, the isoflavones combination also had a significant tumor-suppressive effect in nude mice (38).

Syrian hamster embryo (SHE) cell growth is inhibited by phytoestrogens (DAI, GEN, BCA) in a concentration-related manner. The growth inhibitory effect of the compounds is ranked: GEN > BCA > DAI, which does not correspond to their apoptosis-inducing abilities. Morphological transforming in SHE cells is elicited by the three phytoestrogens. The transforming activities are ranked as follows: GEN > DAI >BCA. Somatic mutations in SHE cells at the Na+-K+-ATPase and hprt loci are induced by GEN or DAI. Chromosome aberrations are induced by GEN and aneuploidy in the near diploid range is occurred by GEN or BCA. GEN, BCA or DAI induce DNA adduct formation in SHE cells with the abilities: GEN > BCA > DAI. The three phytoestrogens induce cell transformation in SHE cells and the transforming activities of these phytoestrogens correspond to at least 2 of the mutagenic effects, i.e., gene mutations, chromosome aberrations, aneuploidy or DNA adduct formation, suggesting the involvement of mutagenicity in the initiation of phytoestrogen-induced carcinogenesis (39).

A nonrandomized, nonblinded trial was performed with historically matched controls from archival tissue designed to determine the effects of acute exposure to a dietary supplement of isoflavones in men with clinically significant prostate cancer before radical prostatectomy. Thirty-eight patients were recruited to the study upon diagnosis of prostate cancer. Before surgery, 20 men consumed 160 mg//day of red clover-derived dietary flavones, containing a mixture of GEN, DAI, formononetin, and BCA. Serum PSA, testosterone, and biochemical factors were measured, and clinical and pathological parameters were recorded. The incidence of apoptosis in prostate tumor cells from radical prostatectomy specimens was compared between 18 treated and 18 untreated control tissues. There are no significant differences between pre- and posttreatment serum PSA, Gleason score, serum testosterone, or biochemical factors in the treated patients ($p > 0.05$). Apoptosis in radical prostatectomy specimens from treated patients was significantly higher than in control subjects ($p = 0.0018$), specifically in regions of low to moderate grade cancer (Gleason grade 1-3). No adverse events related to the treatment are reported (40).

For GEN, BCA and apigenin, reported mechanisms for the biological activities are numerous and include regulation of estrogen-mediated events, inhibition of tyrosine kinase and DNA topoisomerase activities(41), synthesis and release of TGFbeta, and modulation of apoptosis. However, the biochemical effects of GEN in cell culture occur at concentrations in the micromolar range, far above the circulating levels of the unconjugated GEN. The may point to the limitations of cell culture for the evaluation of the activity and mechanisms of potential anti-carcinogens. GEN is extensively metabolized in vivo, with only about 14-16% excreted in an unmodified form. Metabolism may also occur because of interactions between GEN (as well as other polyphenols) and oxidants produced by inflammatory cells (HOCl, HOBr and ONOO-. These react with GEN to form brominated, chlorinated and/or nitrated GEN. Emerging evidence indicates that these modifications may substantially increase the biological activities of the parent compound (42).

BCA treatment induces dose- and time-dependent inhibition on MCF-7 human breast cancer cell line growth at concentrations above 20 µg/ml. An examination of treated MCF-7 cell morphology reveals condensation of the chromosome and dehydration of the cytoplasm, suggesting apoptosis as an important factor in BCA-related cell growth inhibition. At concentration of 40 µg/ml, BCA also decreases the levels of inducible nitric oxide synthase, thus inhibiting the production of nitric oxide, a known second messenger and inducer of apoptosis (43). GEN inhibits MDA-MB-468 human breast cancer cell growth with IC50 value of 8.8 µM, while DAI is less effective. Flow cytometric analysis showed G2/M cell cycle arrest with 25 µM and higher concentrations of GEN. At 100 µM, GEN causes accumulation of 70% cells in G2/M phase by 24 h. In contrast, BCA and DAI are ineffective. APO-BRDU analysis reveals apoptosis with 10 µM GEN (19.5%), reaching 86% at 100 µM. Apoptosis by GEN is confirmed by Hoechst 33342 staining and fluorescence microscopy. GEN treatment results in a biphasic response on cyclin B1: 70% increase in cyclin B1 level at 25 µM, and 50 and 70% decrease at 50 and 100 µM, respectively. GEN has no effect on cdc2 level up to 50 µM concentration; however, there is a decrease in the phosphorylated form of the protein at 100 µM (44).

Cooperative actions of GEN, DAI and BCA is more effective in growth inhibition and apoptosis induction of G2-M cell cycle arrest and an inhibition of cdc2 kinase activity. Both DAI and BCA directly induce apoptosis without altering cell cycle distribution. The IC50 levels of non-transformed immortalized uroepithelial cell line are higher than those in most bladder cancer cell lines, and the IC50 of the mixture regimen is within reach of the levels observed in urine after a soy challenge. Furthermore, both GEN and combined isoflavones exhibit a significant tumor suppressor effect in severe combined immunodeficient mice ($p < 0.05$) (45).

Pure soy isoflavones (GEN, DAI and BCA) and soy phytochemical concentrate exhibit dose-dependent growth inhibition of murine (MB49 and MBT-2) and human (HT-1376, UM-UC-3, RT-4, J82 and TCCSUP) bladder cancer cell lines. Soy isoflavones induce a G2/M cell cycle arrest in all human and murine cell lines evaluated by flow cytometry. In addition, some bladder cancer cell lines show DNA fragmentation consistent with apoptosis. Soy products reduce angiogenesis, increase apoptosis, and slightly reduce proliferation while showing no histopathological on normal bladder mucosa in vivo (46).

Proliferation of HSC-41E6, HSC-45M2, and SH101-P4 stomach cancer cell lines was strongly inhibited by BCA and GEN, whereas other stomach, esophageal, and colon cancer cell lines are moderately suppressed by both compounds. BCA and GEN are cytostatic at low concentration (<20 mg/ml for BCA, <10 mg/ml for GEN) and are cytotoxic at higher concentrations (>40 mg/ml for BCA and <20 mg/ml for GEN). DNA fragmentation is observed at cytotoxic doses of both compounds, indicating the apoptotic mode of cell death. Chromatin condensation and nuclear fragmentation of each cell line are also observed. The advent of apoptosis is dose dependent for both isoflavones. BCA suppressed tumor growth of HSC-45M2 and HSC-41E6 cells in athymic nude mice (47).

Puerarin

Puerarin, PUE, (7-hydroxy-3-(4-hydroxyphenyl)-1-benzopyran-4-one, 8-(beta-D-glucopyranoside)), the main isoflavone glycoside from Chinese herb radix of *Pueraria lobata* (willd) ohwi, has been used for a various medicinal purpose in traditional Chinese medicine. PUE is the most abundant isoflavone-*C*-glucoside extracted from Pueraria radix and has been shown to have beneficial effects on cardiovascular, neurological, and hyperglycemic disorders. *Pueraria mirifica* also possesses estrogenic effect and could inhibit MCF-7 cell growth at high concentration as other flavonoids. Modern pharmacological researches have demonstrated that puerarin exerts a protective effects against myocardial reperfusion injury (48) and ischemic retinopathy (49). PUE also has antihyperglycemic effect by increasing insulin sensitivity and has been clinically used for the therapy of diabetes mellitus and its complication (50). Besides its hypoglycemic effect, PUE has been shown to possess antioxidant properties such as scavenging reactive oxygen species, increasing superoxide dismutase (SOD) activity and inhibiting protein nonenzymatic glycation (51).

Apigenin

Apigenin (4',5,7-trihydroxyflavone), a flavone subclass of flavonoid widely distributed in many herbs, fruits, and vegetables is a substantial component of human diet and has been shown to possess a variety of biological activities including tumor growth inhibition and chemoprevention. Flavonoids have beneficial activities which modulate oxidative stress, allergy, tumor growth and viral infection, and which stimulate apoptosis of tumor cells. In addition to these activities, dietary flavonoids are able to regulate acute and chronic inflammatory response. There are many reports about the actions of apigenin on cancer cell apoptosis such as followings.

Treatment with apigenin or API (0, 20, 40, 60, and 80 microM) for 48 h results in reduction in cell number concurrent with flow cytometry results showing a dose-dependent accumulation of cells in the G2/M phase in both HT29-APC (adenomatous polyposis coli) and HT29-GAL (beta-galactosidase) cells without ZnCl2 treatment.

Flow cytometric analysis showed an increase in the percentage of cells in G2/M when HT29-APC cells with 80 μM apigenin for 120 h. This increase is not present in HT29-APC cells when treated with both 80 μM apigenin and 100 μM ZnCl2 for 120 h. Western blot analysis shows the induction of APC protein in ZnCL2-treated HT29-APC cells but not in ZnCl2-treated HT29-GAL cells. Apigenin plus ZnCl2 treatment increases the expression of APC protein in HT29-APC cells by 50 fold above expression observed with ZnCl2 alone. Upon induction of the APC gene with ZnCl2 in HT29-APC cells, the percentage of apoptotic cells increases significantly after 120-h treatment. Apigenin treatment (80 μM) further increases the percentage of apoptotic HT29-APC cell Following ZnCl2 treatment to induce wild type APC expression (52). Apigenin, a dietary flavonoid derived from plants and vegetables, inhibits keratinocyte differentiation by suppressing MAPK signal transduction and reducing AP-1 transcription factor level. It also inhibits keratinocyte proliferation (53).

ABCC1 expression in tumor cells correlates with their hypersensitivity to various glutathione modulating agents, as demonstrated in H69AR-drug selected and GSH synthesis with BSO or by increasing ABCC1-mediated GSH transport with verapamil or apigenin. It also shows that the hypersensitity of ABCC1-expressing cells to BSO, verapamil or API is preceded by an increase in reactive oxygen species (ROS). The hypersensitivity to BSO, verapamil or API leads to tumor cell death by apoptosis (54).

Actively growing SQ-5 cells, which are derived from a human lung carcinoma, are incubated for 16 h at 37 degrees Celsius in medium containing API 40 μM. The cells are then irradiated with X-rays and incubated with API for a further 8 h. Radiosensitivity is assessed using a clonogenic assay. Apoptosis and necrosis are assessed using acridine orange/ethidium bromide double staining. Cells incubated with API exhibits significantly greater radiosensitivity and apoptosis levels than cells not incubated with API. Incubating with API increases protein expression of SQ-5 spheroids (cell aggregates growing in a three-dimensional structure that simulate the growth and microenvironmental conditions of in vivo tumors) to radiation (55).

Treatment with flavonoids such as apigenin and genistein, resulted in significant downregulation of LPS-elicited TNF-alpha and nitric oxide (NO) production and diminished lethal shock. In chronic diseases, pathogenesis of collagen-induced arthritis (CIA), a mouse model of rheumatoid arthritis which is triggered by TNF-alpha, is improved by the oral administration of flavonoids after the onset of CI. The inhibitory effects of flavonoids on acute and chronic inflammation are due to regulation of signaling pathways, including NF-kappaB activation and MAPK family phosphorylation. FcetaRI expression by NF-kappaB activation is also reduced by flavonoids; while accumulation of lipid rafts, which is the critical step for signaling, is blocked by flavonoids. The intake of dietary flavonoids reduces acute and chronic inflammation due to blocking receptor accumulation and signaling cascades, and would assist individuals at high-risk from life-style related diseases (56)

It has been recently shown that API inhibits hypoxia-inducible factor-1 (HIF-1) and vascular endothelial growth factor (VEGF) expression in human ovarian cancer cells under normoxic condition. Angiogenesis is the formation of new blood vessels and is required for tumor growth and metastasis. API inhibits expression of HIF-1 and VEGF in different cancer cells under both normoxic and hypoxic conditions. API significantly inhibits tumor angiogenesis in vivo, by using both the chicken chorioallantoic membrane and Matrigel plug assays. The inhibition of tumor angiogenesis is associated with the decrease of HIF-1 and VEGF in tumor tissues. Hence, API suppresses tumor angiogenesis through HIF-1 and VEGF expression (57).

Apigenin markedly induces the expression of death receptor 5 (DR5) and syngergistically acts with exogenous soluble recombinant human tumor necrosis factor-related apoptosis-inducing ligand (TRAIL) to induce apoptosis in malignant tumor cells. TRAIL is a promising candidate for cancer therapeutics due to its ability to selectively induce apoptosis in cancer cells. The combined use of apigenin and TRAIL at suboptimal concentrations induces Bcl-2-interacting domain cleavage and the activation of caspases-8, -10, -9, and -3. Furthermore, human recombinant DR5/Fc chimera protein and caspase inhibitors dramatically inhibit apoptosis induced by the combination of apigenin and TRAIL. On the other hand, apigenin-mediated induction of DR5 expression is not observed in normal human peripheral blood mononuclear cells. Moreover, apigenin does not sensitize normal human peripheral blood mononuclear cells to TRAIL-induced apoptosis (58).

Apigenin induces human gastric carcinoma SGC-7901 cells to die via apoptosis in a dose-dependent manner (18). Apigenin exhibits a significant growth inhibition against the three hepatoma cell lines, i.e., Hep G2, Hep 3B, and PLC/PRF/5 cells, but not the normal murine liver BNL CL.2 cells. Using DNA ladder and flow cytometric analysis, apigenin induces apoptosis in Hep G2 cells. It also increases the accumulation of p53 and enhanced the level of p21/WAF1, which is associated with the cell cycle arrest in G2/M phase (59)

Apigenin inhibits A549 lung cancer cell proliferation and vascular endothelial growth factor (VEGF) transcriptional activation in a dose-dependent manner. It inhibits VEGF transcriptional activation through hypoxia-inducible factor-1 (HIF-1) binding site and specifically decreases HIF-alpha but not HIF-beta subunit expression in the cells. Apigenin inhibits AKT and p70S6K1 activation. It also inhibits tumor growth in nude mice. Apigenin inhibits HIF-1alpha and VEGF expression in the tumor tissues, suggesting an inhibitory effect on angiogenesis which is confirmed by Matrigel assay (60).

Apigenin is much more potent than kaempferol at: (1) inhibiting chymotrypsin-like activity of purified 20S proteasome and of 26S proteasome in intact leukemia Jurkat T cells; (ii) accumulating putative ubiquitinated forms of two proteasome target proteins, Bax and inhibitor of nuclear factor kappabeta-alpha in Jurkat T cells and (iii) inducing activation of caspase-3 and cleavage of poly(ADP-ribose) polymerase in Jurkat T cells. The proteasome-inhibitory ability is correlated with their apoptosis-inducing potency. Finally, apigenin neither effectively inhibits the proteasome activity nor induces apoptosis in non-transformed human natural killer cells (61).

Apoptosis

In mammalian cells, there are two major pathways involved in apoptosis: the mitochondria-initiated intrinsic pathway and the death receptor-stimulated extrinsic pathway (62-64). For the former, proapoptotic signals provoke cytochrome c release from the mitochondrial intermembranous space into the cytosol, which forms a complex with Apaf-1 and dATP, known as an apoptosome, and triggers caspase-9 activation. The activation of caspase-9 leads to the activation of the executioner caspases, such as caspase-3, -6, -7, which stimulates a series of apoptotic events, eventually leading to cell death (62, 65, 66). The extrinsic pathway begins with the death receptors, such as Fas. When Fas ligand binds to the Fas death receptor, the adaptor molecule is recruited to the receptor, which allows the binding and proteolysis of caspase-8 to activate the caspase-8. The activated caspase-8 then cleaves the effector caspase-3, -6 and -7, leading to cell death (63, 65, 67).

Endoplasmic reticulum (ER) stress

The endoplasmic reticulum (ER) regulates protein synthesis and intracellular calcium (Ca^{2+}) homeostasis (68). Excessive ER stress can trigger apoptosis through a variety of mechanisms including redox imbalance, alteration in Ca^{2+} levels and activation of Bcl-2 family proteins (69). Thapsigargin (THG), a sesquiterpenoid plant alkaloids, is frequently used to study the mechanisms regulating ER-stress-induced apoptosis in cancer cell lines via activation of the death receptor pathway and the mitochondrial pathway (70).

Calreticulin (CRT) is an abundant Ca^{2+}-binding chaperone, which is mostly present in the endoplasmic reticulum (ER) lumen, although it can also be found in other subcellular localization (71, 72). When present on the surface of damaged cells, it can serve as an 'eat-me' signal and hence facilitate the recognition and later engulfment of the dying cells by macrophages (73) or by dendritic cells (74). It is thought that this function determines the immunostimulatory effect of CRT, because presentation of tumor antigens by dendritic cells is indeed required for the immunogenic effect of anthracyclin-treated cancer cells (74-76). Alternatively or in addition, CRT may bind antigenic peptides from tumor and facilitate their efficient presentation to T cells (77).

Despite extensive analysis of anti-tumor activities of ZEA, its ability to moderate leukemic cell growth has not yet been well characterized. We used two human leukemic cell lines (HL-60 and U937) to study the apoptotic effect of ZEA and the underlying mechanism. It was found that human leukemic cell apoptosis induced by ZEA was related to caspase-3 activity, MTP reduction and cytochrome c release, which are the mitochondrial pathway. ZEA induced oxidative stress via ROS generation. The mechanistic effect also involves Ca^{2+} concentrations in cytosol and mitochondria indicating ER stress but there is no calreticulin exposure on the cell membrane.

MATERIALS AND METHODS

Chemicals

Nine phytoestrogens, i.e., baicalein (BAI), bisphenol A (BPA), naringenin (NAR), zearalenone (ZEA), genistein (GEN), apigenin (API), biochannin A (BCA), puerarin (PUE), daidzein (DAI) were obtained from Sigma, St. Louis, MO, USA, and their structures are shown in Fig. 1. RPMI-1640 and fetal bovine serum were obtained from Gibco-BRL, New York, NY, USA, propidium iodide (PI), 3,3'-dihexyloxacarbocyanine idodide ($DiOC_6$), and 2'7'-dichlorofluorescein diacetate (DCFH-DA) from Sigma, St. Louis, MO, USA.

Cell culture

Human promyelocytic leukemic cells HL-60 and human promonocytic U937 cells were cultured in 10% fetal bovine serum in RPMI-1640 medium (Invitrogen, USA) supplemented with penicillin G (100 units/ml) and streptomycin (100 μg/ml) at 37°C in a humidified atmosphere containing 5% CO_2. The preconfluent (growth phase) HL-60 cells or U937 cells ($1x10^6$ cells) were treated with ZEA at indicated concentrations.

Peripheral blood mononuclear cells (PBMCs) were isolated from heparinized blood obtained from adult volunteers by density gradient centrifugation using lymphoprep (Sigma, St. Louis, MO, USA), according to standard protocols. After separation, cells were cultured in RPMI-1640 medium supplemented with 10% heat-activated fetal bovine serum, 2 mM glutamine, 100 U/ml penicillin, and 100 μg/ml streptomycin. PBMCs were treated with phytoestrogens at various concentrations.

Cytotoxicity test

MTT assay was performed as described briefely (78). Following phytoestrogens treatment, cell viability was assessed by MTT assay. This method is based on the ability of viable cells to reduce MTT (3-(4,5-dimethyl)-2,5-diphenyl tetrazolium bromide) and form a blue formazan product. MTT solution (sterile stock solution of 5 mg/ml) was added to the incubation medium in the wells at a final concentration of 100 μg/ml and incubated for 4 h at 37 °C in a humidified 5% CO_2 atmosphere. The medium was then removed and plate was shaken with DMSO for 30 min. The optical density of each well was measured at 540 nm with reference wavelength of 630 nm using microtiter plate reader. Number of viable cells was calculated from untreated cells, and the data were expressed as % cell viability.

Fluorescence microscopy

Treated cells were cytospun on glass slides. After air drying, cells were fixed with absolute methanol for 10 min at –20 °C, washed twice with PBS and air-dried. Propidium iodide (PI, Sigma, USA; 200 μg/ml) was applied to the fixed cells for 10 min at room temperature. After washing with PBS and drying, the slides were mounted with 90% glycerol and examined under fluorescence microscope.

Determination of mitochondrial transmembrane potential and ROS production

For measurement of mitochondrial membrane potential and intracellular ROS, either 40 nM of 3,3'-dihexyloxacarbocyanine iodide ($DiOC_6$; Sigma, USA) (for mitochondrial membrane potential) or 5 μM of DCFH-DA (Sigma, USA) (for ROS detection) was added for 15 min at 37 °C and the cells are then subjected to flow cytometry.

For flow cytometric assessment of DNA fragmentation and cell cycle distribution, $1x10^6$ cells were harvested and re-suspended in a solution containing propidium iodide (50 μg/ml), 0.1% Triton X-100, and 0.1% sodium citrate in PBS.

Cells were then analyzed on a FACScan equipped with a 488 nm argon laser using the CellQuest software (Becton-Dickenson, USA). Data were depicted as histograms and the percentage of cells displaying hypodiploid DNA content was indicated. The percentage of cells in each phase was also evaluated to see whether there was cell cycle arrest or not.

Assay of Caspase-3 and caspase-8 activity

Cleavage of the fluorogenic peptide substrates DEVD-AMC (Biosource, USA) and IETD-AMC (Biosource, USA) (indicative of caspase-3-like and caspase-8 like enzyme activity) were estimated. Cell lysates ($1x10^6$ cells) and substrate (50 μM) were combined in a standard reaction buffer and added to a 96-well plate. Enzyme-catalyzed release of AMC was measured using 355 nm excitation and 460 nm emission wavelengths.

Two-dimensional polyacrylamide gel electrophoresis

The albumin was removed by using ProteoExtract Albumin/Removal kit. The amount of protein loaded in 2-D PAGE was 200 μg/gel. 2-D PAGE was performed using the immobiline/polyacrylamide system. Samples were applied by overnight in-gel rehydration of 70 mm (analytical runs) and 180 mm (preparative runs), using nonlinear pH 3–10, IPG gel strips (GE Healthcare, Uppsala, Sweden). The first dimension (IEF) was performed at 6500 V.h for 3.5 h, using a Pharmacia LKB Multiphor II system. The IPG strips were equilibrated in two steps of equilibration buffer. The first step employed 50 mM Tris-HCl buffer, pH 6.8, 6 M urea, 30% glycerol, 1% SDS, and 1% DTT, while 2.5% iodoacetamide replaced DTT in the second step. The IPG strips were then applied to the second-dimension 12.5% T SDS polyacrylamide gels (100 mm x 80 mm x 1.5 mm). Electrophoresis of the minigel was performed in a Hoefer system at 20 mA, room temperature for 2 h. After electrophoresis, proteins were visualized by CBR-250 staining or SYPRO Ruby staining.

Western blot analysis

To separate the cytosolic-rich fraction, cells treated with zearalenone were harvested and washed once in ice cold PBS and incubated at 4°C for 10 min with ice-cold cell lysis buffer (250 mM Sucrose, 70 mM KCl, 0.25% Triton X-100, 100 μM PMSF, 1 mM DTT in PBS with protease inhibitors). The cell suspension was centrifuged at 20,000 x *g* for 20 min. The supernatant was collected and kept as the cytosolic-rich fraction. The protein concentration of the lysates was determined by the Bradford method, using BSA as standard. Cellular protein (50 μg protein) were separated by electrophoresis on 17% SDS-PAGE and transferred onto nitrocellulose membranes. After blocking in 5% non-fat milk in TBS containing 0.2% Tween-20, blots were incubated with mouse monoclonal antibodies to cytochrome c, Bax, Bcl-2 and rabbit polyclonal antibody to Bcl-xL (Abcam, Cambridge, UK). For detection the appropriate horseradish peroxidase (HRP) conjugated second antibodies (Abcam, Cambridge, UK) were used at 1:20,000 dilution. Protein bands were visualized with SuperSignal West Pico Chemiluminecent Substrate (Pierce, Rockford, IL, USA) on X-ray film.

FACS analysis for cytosolic and mitochondrial Ca^{2+} levels

Cytosolic Ca^{2+} levels were determined using the fluorescence dye 1 μM Fluo3-AM (Molecular Probes, Eugene, OR, USA) in FITC setting. Mitochondrial Ca^{2+} levels were determined using the fluorescent dye 250 nM Rhod2-AM (Molecular Probes, Eugene, OR, USA) in PE setting. After cells were treated with ZEA for 4 h, the cells were incubated with fluorescence dye for 15 min at 37 °C, and washed with

PBS containing 10 mM glucose and analyzed immediately by flow cytometry. In each analysis, 10,000 events were recorded.

Flow cytometric analysis of calreticulin on the cell surface

HL-60 cells were plated in 24-well plates and incubated for indicated time. Cells were harvested, washed twice with PBS and incubated for 30 min with primary antibody, diluted in cold blocking buffer (2% FBS in PBS), followed by washing and incubation with the FITC-conjugated monoclonal secondary antibody diluted 1:500 in blocking buffer (30 min). Each sample was then analyzed by FACScan (Becton Dickinson, USA) to identify cell surface calreticulin. Isotype matched IgG antibodies were used as a control, and the fluorescence intensity of stained cells was gated on propidium iodide (PI) negative cells.

Statistical analysis

Results are expressed as mean $\pm$ SEM (standard error of the mean). Statistical differences between controls and treated groups were determined by the one-way ANOVA (Kruskal Wallis analysis) at limit of $p<0.05$ in triplicate of three independent experiments.

A. Baicalein

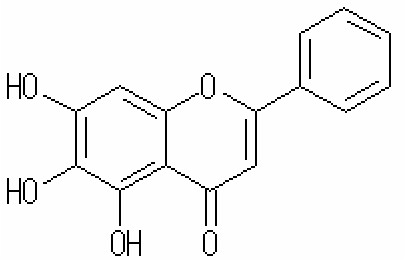

B. Bisphenol A

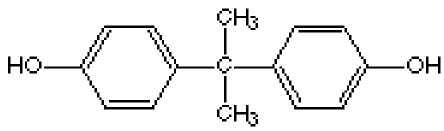

Bisphenol A

C. Naringenin

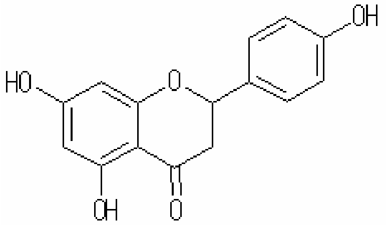

D. Zearalenone

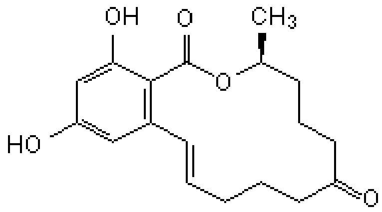

E. Genistein

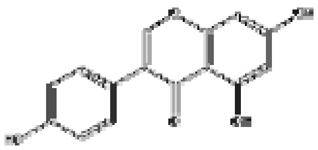

F. Apigenin

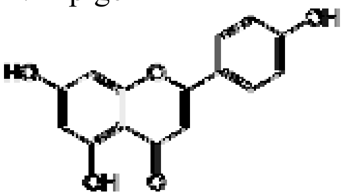

G. Biochannin A

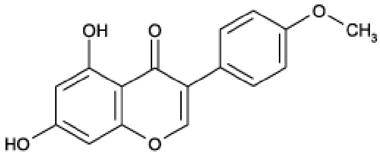

H. Puerarin

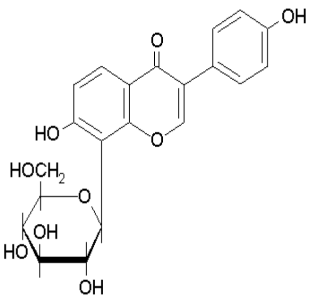

I. Daidzein

Fig. 1 The structure of nine phytoestrogens.

RESULTS AND DISCUSSION

All phytoestrogens, except PUE and DAI, were toxic to HL-60 and U937 cells in a dose dependent manner (Fig. 2). NAR and BCA have the proliferative effect on PBMCs at the lower concentrations as shown in Fig. 2C and 2G. As shown in Fig. 2, the U937 cells were more sensitive to the phytoestrogens in the order of U937 > HL-60 > PBMCs in all phytoestrogens except BPA which HL-60 was sensitive in the same degree compared to PBMCs (Fig. 2B). The most cytotoxic phytoestrogens was API and ZEA, of which the IC_{50} levels toward U937 cells were 12 and 16 µM, respectively. Puerarin and daidzein were the least toxic to all cells (Fig. 2H and Table 1).

Pure soy isoflavones (genistein, daidzein, biochannin A) exhibit dose-dependent growth inhibition of murine (MB49 and MBT-2) and human (HT-1376, UM-UC-3, RT-4, J82, and TCCSUP) bladder cancer cell lines, although the degree of inhibition varies among lines. Soy products reduce angiogenesis, increase apoptosis, and slightly reduce proliferation while showing no histopathological effects on the normal bladder cells (46).

Naringenin (NAR), a flavonoid, has shown cytotoxicity in various human cancer cell lines and inhibitory effects on tumor growth. Exposure of HL-60 cells to NAR induces apoptosis dose-dependently up until 0.5 mM, but not at 1 mM as demonstrated by a quantitative analysis of nuclear morphological change and flow cytometirc analysis (19). Whereas genistein (GEN) and biochannnin A (BCA) exhibit dose-dependent inhibition of growth of AT6.3 rat prostate cancer cell line with IC_{50} between 25 and 40 µM, whereas daidzein (DAI) is less potent with IC_{50} > 60 µM (36).

A character of apoptotic cells via mitochondria is the decrease in mitochondrial transmembrane potential (MTP). It was found that all phytoestrogens except PUE and DAI showed dose response of the changing in TMP significantly compared to control of tested cells (U937 cells and HL-60 cells) as shown in Fig. 3.

The phytoestrogen treated U937 cells cause the increase in reactive oxygen species (ROS) generation following treatment with ZEA, NAR, BPA, BCA, BAI, and PUE as in Fig. 4A and 4B. While in HL-60 cells, the phytoestrogens, i.e., ZEA, NAR and PUE caused the increase of ROS (Fig. 4C). It was reported that phytochemical compounds cause ROS generation and apoptosis in cancer cells such as curcumin (79, 80), which corresponds to the present study. BPA also induces reactive oxygen species and apoptosis in mesencephalic neuronal cells (9).

Table 1 IC_{50} of each phytoestrogen when incubated in U937 and HL-60 cell lines and peripheral blood mononuclear cells (PBMCs)

phytoestrogens	U937 cells*	HL-60 cells (µg/ml)	PBMCs (µg/ml)
API	12	>80	>80
BAI	57	>80	>80
BIO	29	78	>80
BPA	25	65	63
DAI	>80	>80	>80
GEN	23	>80	>80
NAR	104	220	>250
PUE	>80	>80	>80
ZEA	16	44	>80

* µg/ml except ZEA in µM for U937 cells (16 µM or 5.1 µg/ml)

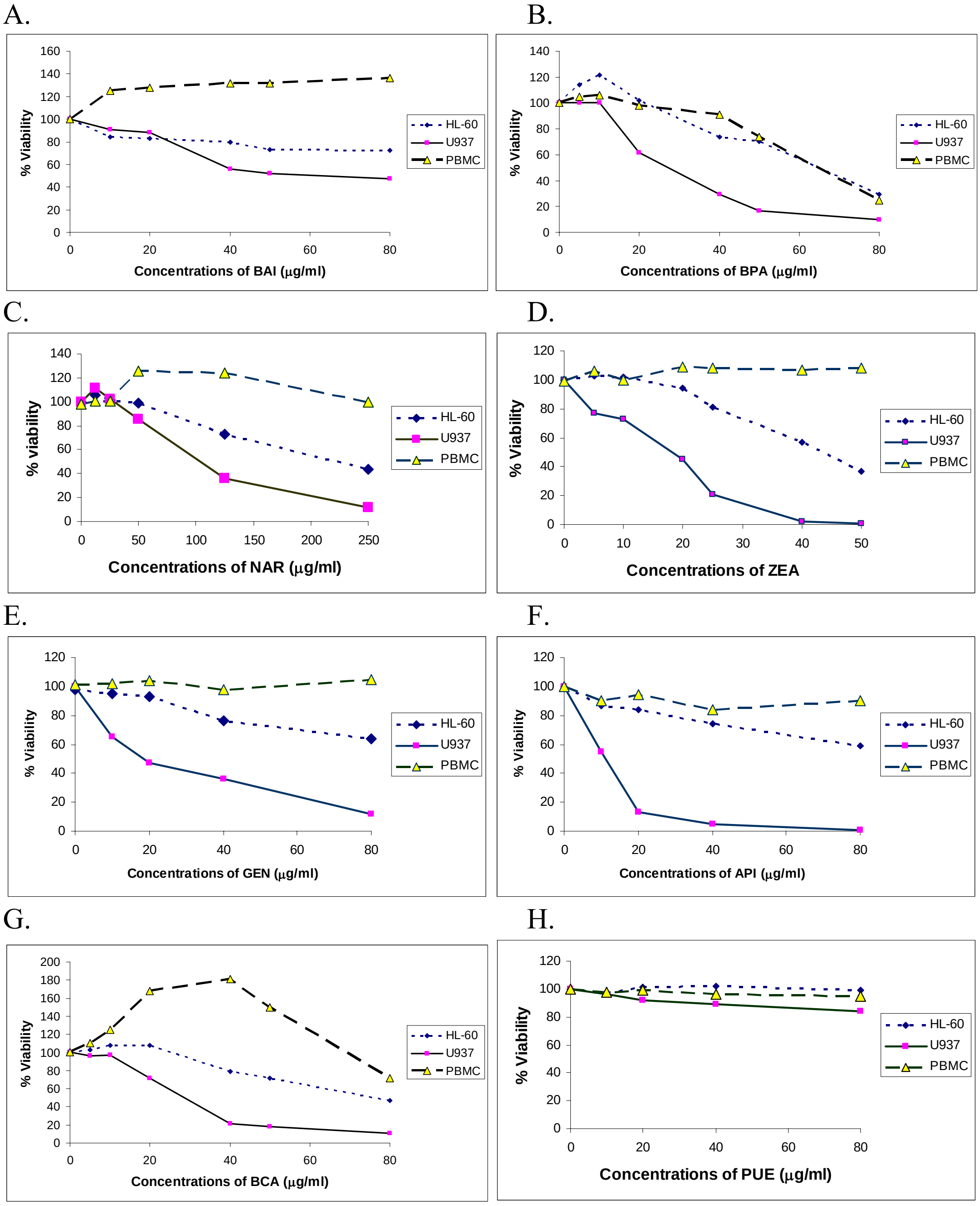

Fig. 2 The effect of phytoestrogens on cell proliferation and cytotoxicity on HL-60, U937 and peripheral blood mononuclear cells. Cells viability was monitored at indicated concentrations of (A) BAI, (B) BPA, (C) NAR, (D) ZEA, (E) GEN, (F) API, (G) BCA and (H) PUE using the MTT assay. Optical absorbance of the reaction was measured spectrophotometrically at 570 nm with ELISA plate reader. The results shown are the average of three different experiments performed in triplicate (bars of SD were not showed).

A.

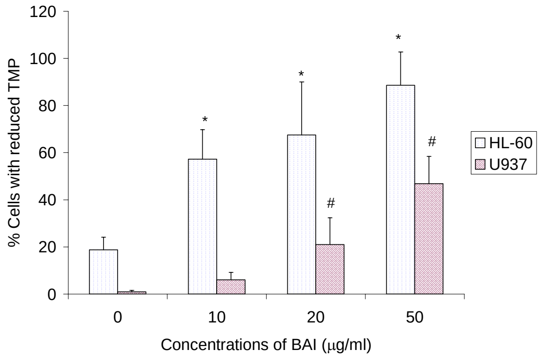

B.

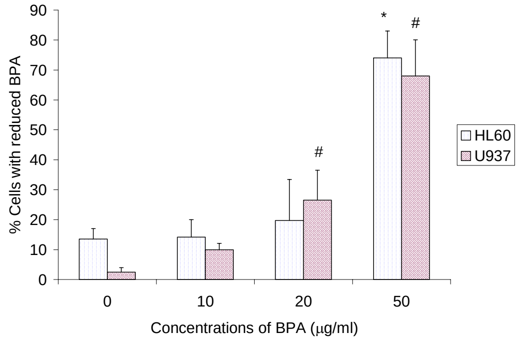

C.

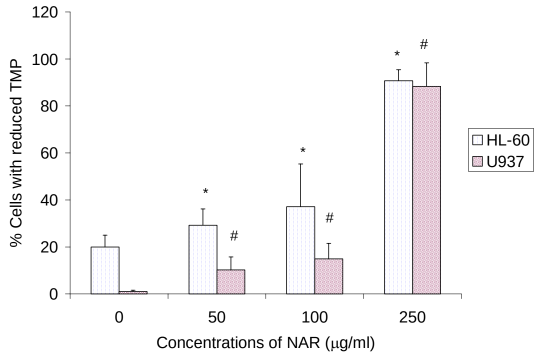

D.

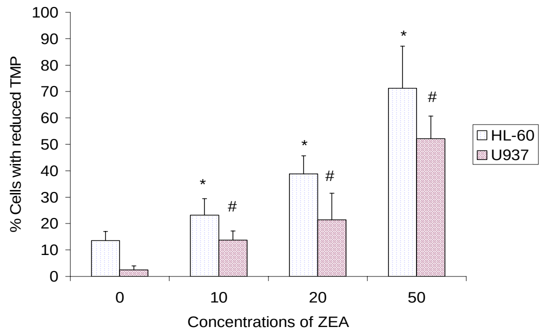

E.

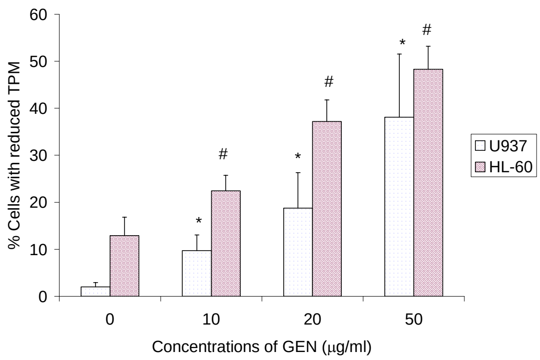

F.

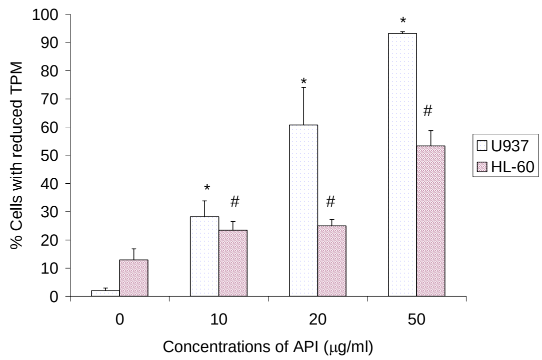

G.

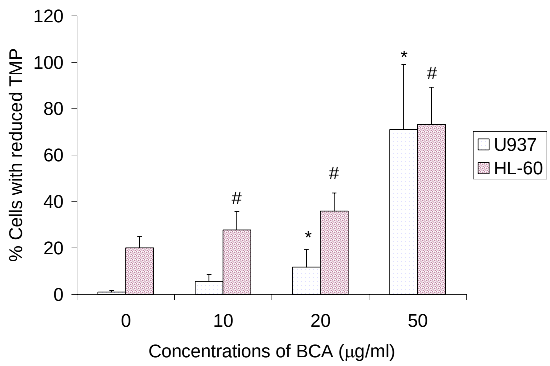

Fig. 3 Dose-response of BAI treatment on reduction of TMP of HL-60 and U937 cells. Cells were treated for 24 h with various concentrations of (A) BAI, (B) BPA, (C) NAR, (D) ZEA, (E) GEN, (F) API and (G) BCA in μg/ml all except of ZEA in U937 cells in μM, incubated with 40 nM of $DiOC_6(3)$ for 15 min and subjected to flow cytometry. Percent cells with decreased TMP are plotted against BAI concentration. Mean and SEM of 3 independent experiments in duplicate are shown.

(* and #) indicates significant difference. BAI: baicalein, BPA: bisphenol A, NAR: naringenin, ZEA: zearalenone, GEN: genistein, API: apigenin and BCA: biochannin A, TMP: transmitochondrial membrane potential.

A.

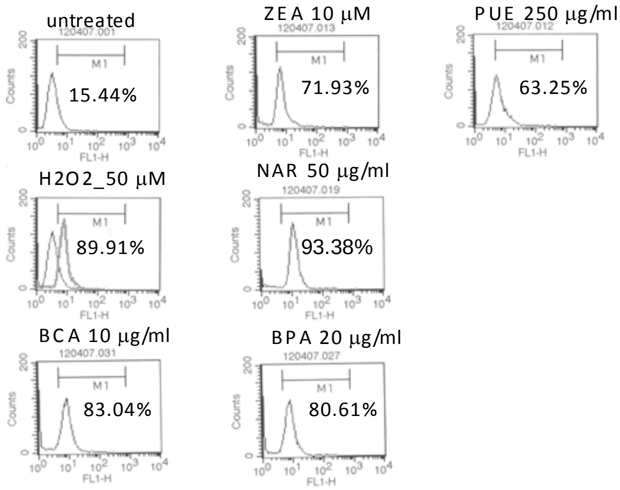

B.

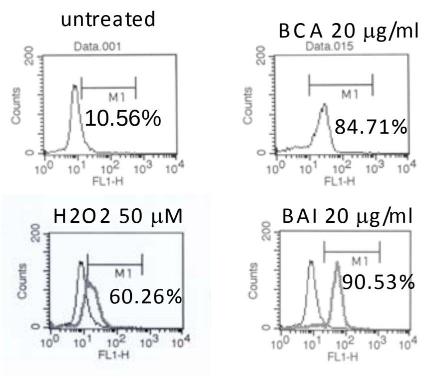

C.

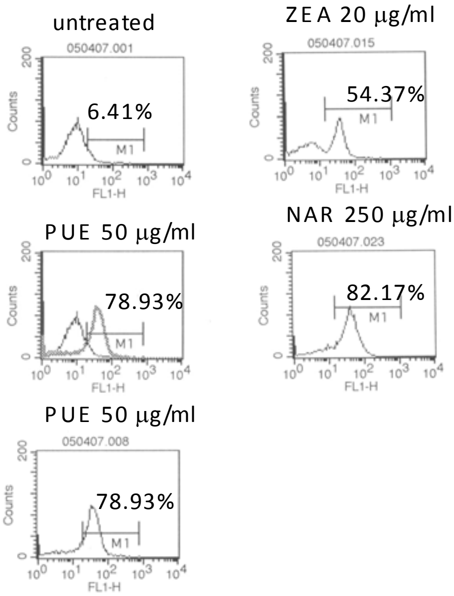

Fig. 4 Generation of reactive oxygen species (ROS) in U937 and HL-60 cells by various phytoestrogens. U937 (A, B) and HL-60 (C) cells were treated with 50 µM of H2O2 (positive control) each phytoestrogen at indicated concentrations for 4 h, incubated with 5 µM of DCFH-DA for 15 min and subjected to flow cytometry and cells with increased fluorescence, indicating the presence of ROS, are located in the region designated M1. ZEA: zearalenone, NAR: naringenin, BAI: baicalein, BPA: bisphenol A, BCA: biochannin A, PUE: puerarin.

BPA caused apoptosis in cultured rat Sertoli cells (10) and central neural cells during early development of *Xenopus laevis* (11). BPA induces apoptosis and G2/M arrest of ovarian granulose cells (12). In the present study, the nucleoids of HL-60 and U937 human leukemic cells were compared when treated with phytoestrogens. In HL-60 cells, BAI (50 µg/ml), BPA (50 µg/ml), NAR (250 µg/ml), ZEA (50 µg/ml), GEN (50 µg/ml), API (50 µg/ml), and BCA (50 µg/ml) caused G2/M arrest but ZEA at a lower dose (10 µg/ml) produced G0/G1 arrest as shown in Fig. 5A-5H. In GEN and DAI treated cells, the number of HL-60 cells that contained subdiploid DNA was in a dose response manner (Fig. 6E and 6H). In BPA-treated HL-60 cells, the cells had high proportion of subdiploid nucleoids in a constant value in all concentrations tested (Fig. 6B). Whereas as in U937 cells, the cells treated with BPA, NAR and ZEA and showed a dose response manner of increase in subdiploid peak and G2/M arrest (Fig. 7 and 8). The reduction of TMP and an existence of subdiploid peak of the cell cycle implied that apoptosis was the mode of cell death in these cells.

ZEA has possessed comparative estrogenic activity and can promote the progression of MCF-7 cells through the cell cycle by a decreasing in the G0/G1 phase and by a significant increase in S phase (81, 82).

Apigenin does not inhibit survival of primary sympathetic neurons, suggesting that it is not toxic to nontransformed cells like our study. The mechanism of action of apigenin cytotoxicity seems to involve p53, as it increased the levels of p53 and the p53-induced gene products p21/WAF1/CIP1 and Bax (83). Apigenin-treated HeLa cells are arrested at G1 phase, which s associated with a marked increment of the expression of p21/WAF1 protein (84). Flow cytometry shows that GEN but not BCA or DAI, induces progressive and sustained accumulation of hepatoma cancer cells in the G2/M phase as a result of inhibition of Cdc2 kinase activity (38). However, Genistein causes a dose-dependent induction of G2/M cell cycle arrest and an inhibition of cdc2 kinase activity in bladder cancer cells. Genistein treatment results in a biphasic response on cyclin B1: 70% increase in cyclin B1 level at 25 μM, and 50 and 70% decrease at 50 and 100 μM, respectively. Biochannin A and daidzein, although structurally related to genistein, does not share genistein's mechanism (44). DAI and BCA directly induce urinary tract cancer cell apoptosis without altering cell cycle distribution. The IC_{50} levels of DAI and BCA in non-transformed cells (normal uroepithelium) are higher than those in most cancer cell lines (45). GEN potently induces G2/M cell cycle arrest in rat prostate cancer cells (36). The mechanism of each phytoestrogen on changing the cell cycle in HL-60 and U937 leukemic cells might involve p53, p21 and Bax or inhibition of cdc2 kinase activity or expression of cyclin B1 which requires further exploration.

A.

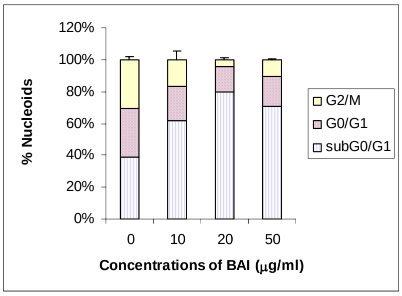

B.

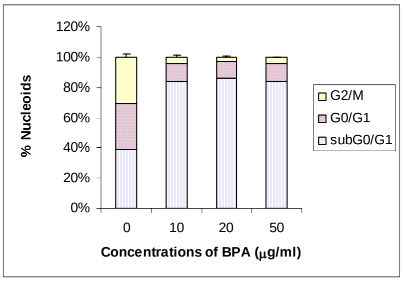

C.

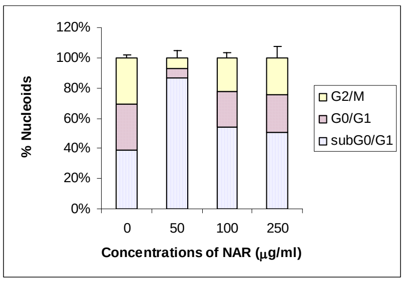

D.

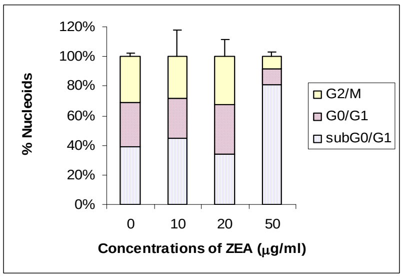

E.

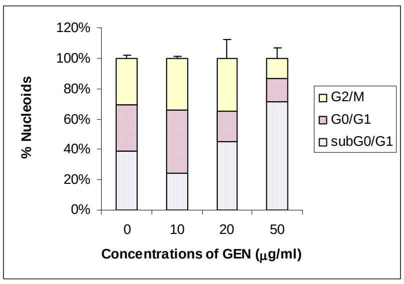

F.

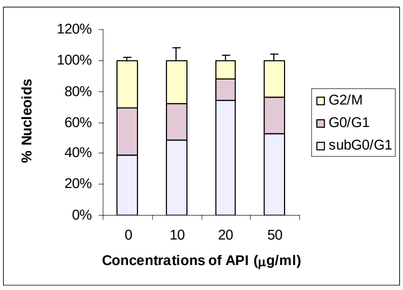

G.

H.

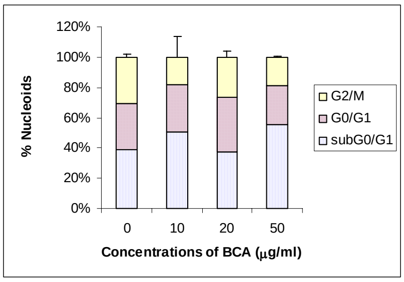

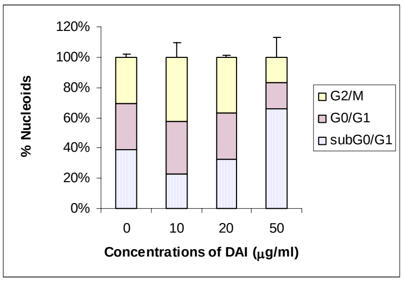

Fig. 5 Cell cycle distribution of HL-60 cells treated with each phytoestrogens. HL-60 cells were treated with (A) BAI, (B) BPA, (C) NAR, (D)ZEA, (E) GEN, (F) API, (G) BCA, or (H) DAI, then stained with propidium iodide and processed by flow cytometry as in materials and methods.

A.

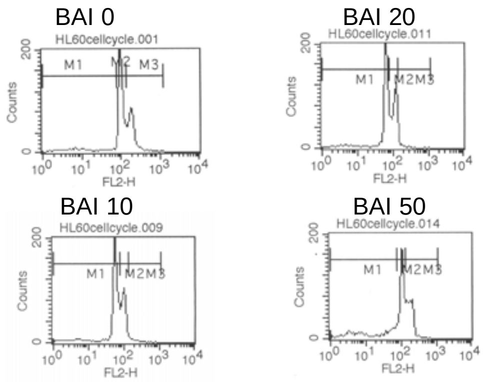

B.

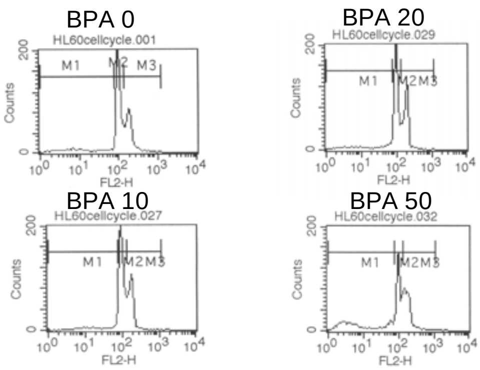
BPA 0
HL60cellcycle.001
BPA 20
HL60cellcycle.029
BPA 10
HL60cellcycle.027
BPA 50
HL60cellcycle.032
M1
M2
M3
Counts
FL2-H

C.

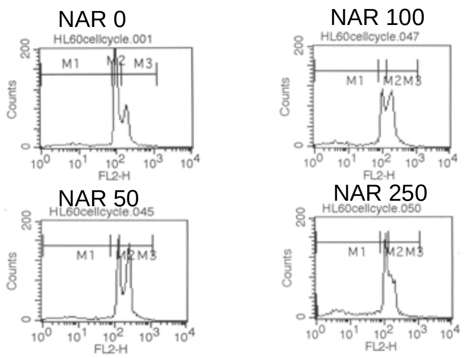
NAR 0
HL60cellcycle.001
NAR 100
HL60cellcycle.047
NAR 50
HL60cellcycle.045
NAR 250
HL60cellcycle.050
M1
M2
M3
Counts
FL2-H

D.

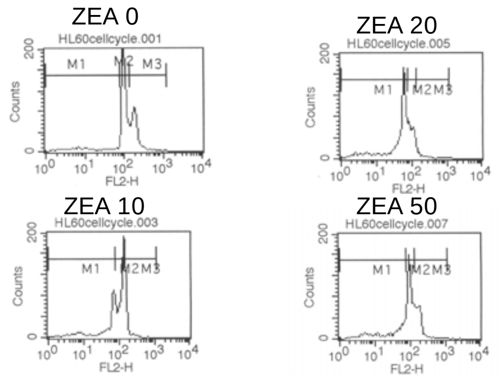
ZEA 0
HL60cellcycle.001
ZEA 20
HL60cellcycle.005
ZEA 10
HL60cellcycle.003
ZEA 50
HL60cellcycle.007
Counts
FL2-H
M1
M2
M3

E.

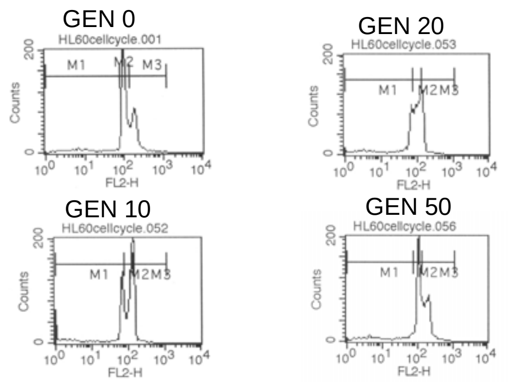
GEN 0
HL60cellcycle.001
GEN 20
HL60cellcycle.053
GEN 10
HL60cellcycle.052
GEN 50
HL60cellcycle.056
Counts
FL2-H
M1
M2
M3

F.

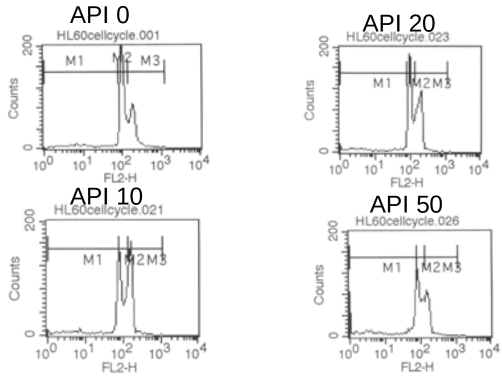
API 0
HL60cellcycle.001
API 20
HL60cellcycle.023
API 10
HL60cellcycle.021
API 50
HL60cellcycle.026
M1
M2
M3
Counts
FL2-H

G.

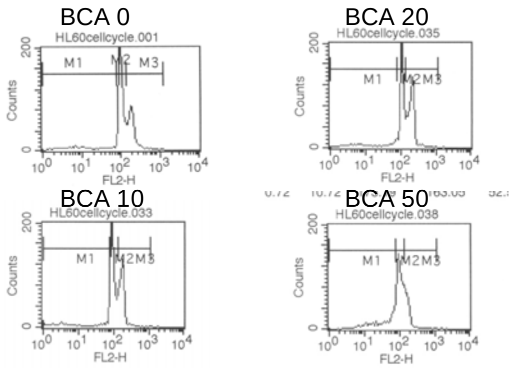
BCA 0
HL60cellcycle.001
BCA 20
HL60cellcycle.035
BCA 10
HL60cellcycle.033
BCA 50
HL60cellcycle.038
M1
M2
M3
Counts
FL2-H

H.

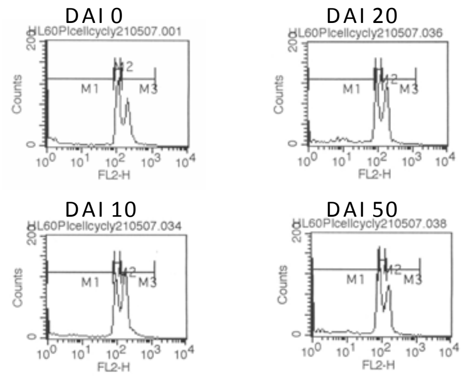

Fig. 6 Cell cycle of HL-60 cells in the conditions of treatment with phytoestrogens. HL-60 cell cycle treated with (A) BAI, (B) BPA, (C) NAR, (D) ZEA, (E) GEN, (F) API, (G) BCA, (H) DAI were shown. The concentrations of each BAI, BPA, NAR, ZEA, GEN, API, BCA are all in μg/ml. Cells were treated with each phytoestrogen for 24 h and then processed and stained with propidium iodide (40 μg/ml) overnight then detected with flow cytometry for cell cycle pattern. BAI: baicalein, BPA: bisphenol A, NAR: naringenin, ZEA: zearalenone, GEN: genistein, API: apigenin, BCA: biochannin A, DAI (daidzein). M1: subdiplid, M2: G0/G1, and M3: G2/M region.

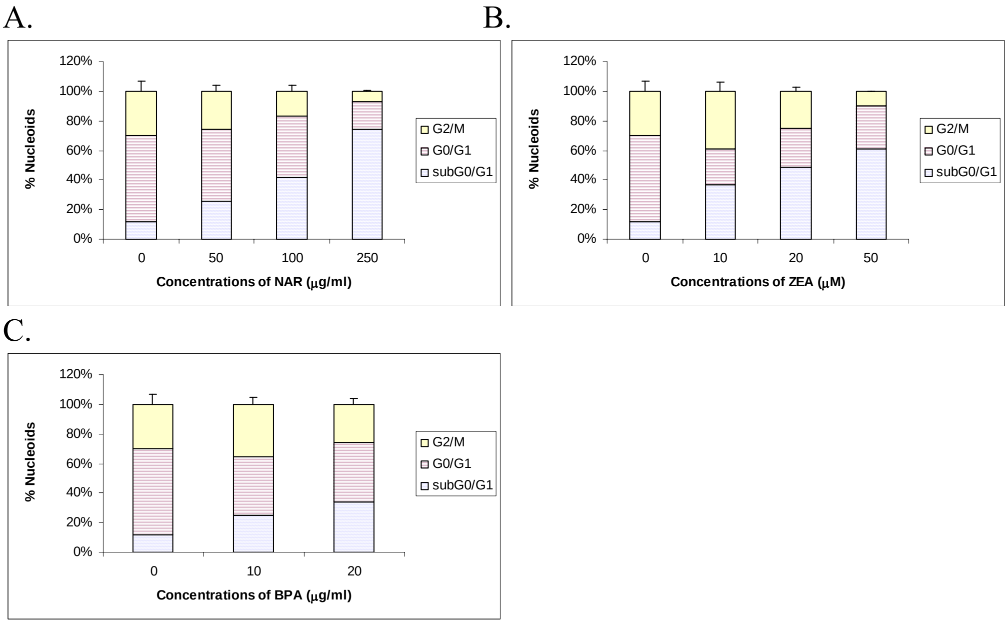

Fig. 7 Cell cycle distribution of U937 cells treated with each phytoestrogens. U937 cells were treated with (A) NAR, (B) ZEA, or (C) BPA, then stained with propidium iodide and processed by flow cytometry as in materials and methods.

A.

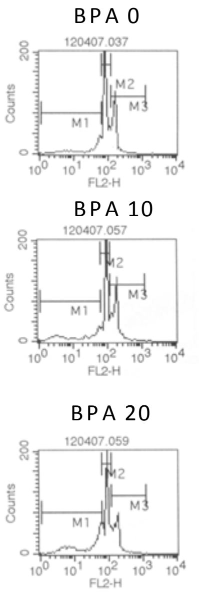
BPA 0
120407.037
BPA 10
120407.057
BPA 20
120407.059
Counts
FL2-H
M1
M2
M3

B.

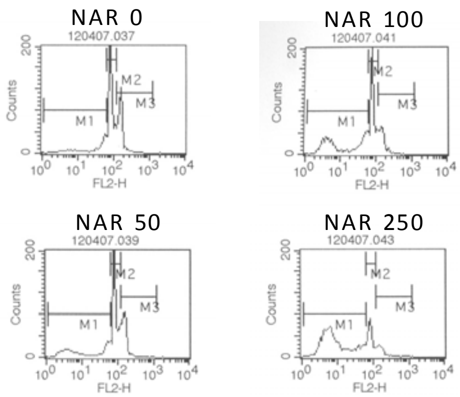
NAR 0
120407.037
NAR 100
120407.041
NAR 50
120407.039
NAR 250
120407.043
Counts
FL2-H
M1
M2
M3

C.

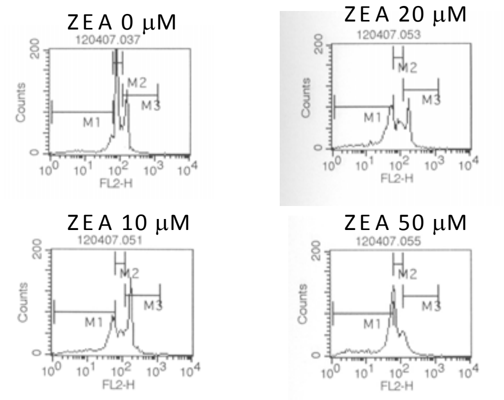

Fig. 8 Cell cycle of U937 cells in the conditions of treatment with phytoestrogens. U937 cells were treated with (A) BPA (B) NAR and (C) ZEA. The concentrations of each BPA and NAR are in μg/ml whereas those of ZEA are in μM. Cells were treated with each phytoestrogen for 24 h and then processed and stained with propidium iodide (40 μg/ml) overnight then detected with flow cytometry for cell cycle pattern. BPA: bisphenol A, NAR: naringenin, ZEA: zearalenone. M1: subdiplid, M2: G0/G1 and M3: G2/M area.

Activation of caspase-3 and cleavage of caspase-3 substrate has also been reported in hepatoma cells, i.e., HepG2, Hep3B, Huh7, PCL and HA22T after 24 h exposure to isoflavones, GEN, BCA and DAI (38). The phytoestrogen-treated U937 cells showed a dose response in caspase-3 activity significantly including BAI, BCA, NAR, BPA and ZEA as shown in Fig. 9A. Similar phenomena occurred in phytoestrogen-treated HL-60 cells, viz. BCA, NAR, BPA and ZEA (Fig. 9B). Such phytoestrogen-treated HL-60 and U937 cell death were caspase-3- and mitochondria-mediated apoptosis.

Concerning zearalenone, no evidence for apoptosis by FACS-analysis for a hypodiploid DNA peak was found after incubation of bovine lymphocytes with 0.1-2 μM ZEA (27), but it was demonstrated that apoptosis occurs in Vero, Caco-2 and DOK cells at concentrations of 10-40 μM ZEA by DNA ladder formation and observations of apoptotic bodies (30). Moreover, ZEA induces cell cycle arrest in these three cell-lines characterized by an increase of the number of cells in G2/M phase (30). ZEA induced apoptosis in rat sperm cells after a single i.p dose of 5 mg/kg which was shown by TUNEL labeling and DNA ladder formation (31). ZEA target mitochondria and /or lysosomes, induces lipid peroxidation, cell death and inhibits protein and DNA syntheses (32). The higher concentration of 30 μg/ml ZEA inhibits T and B lymphocyte proliferation from the stimulation with phytohemagglutinin and pokeweed mitogen. Measurement of ZEA-induced intracellular Ca^{2+} mobilization shows an increase of both Ca^{2+} levels and the number of cells with high Ca^{2+} only in the monocyte/granulocyte gated cells (34).

A.

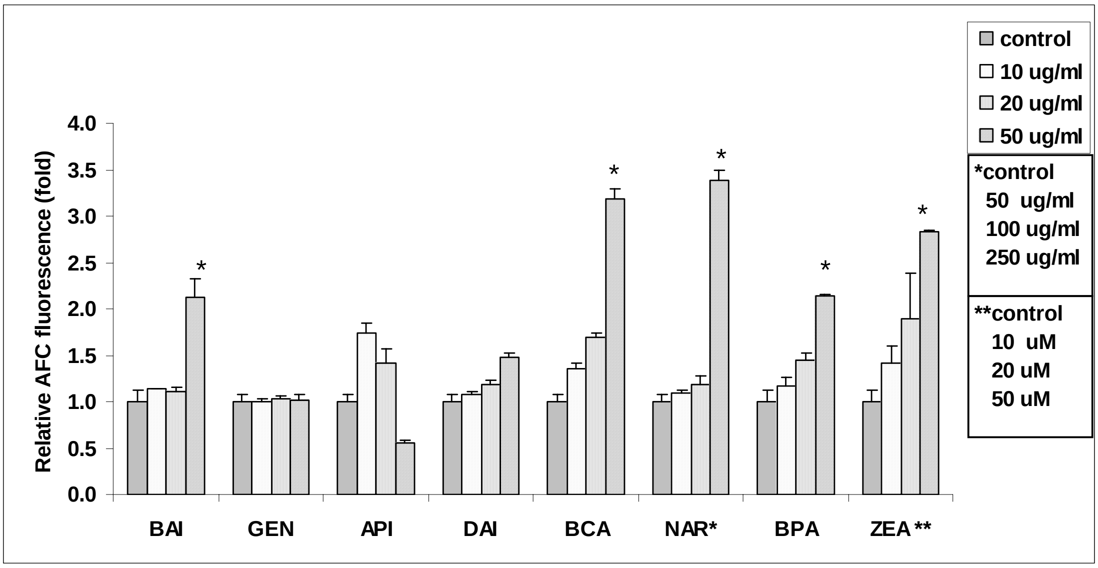

B.

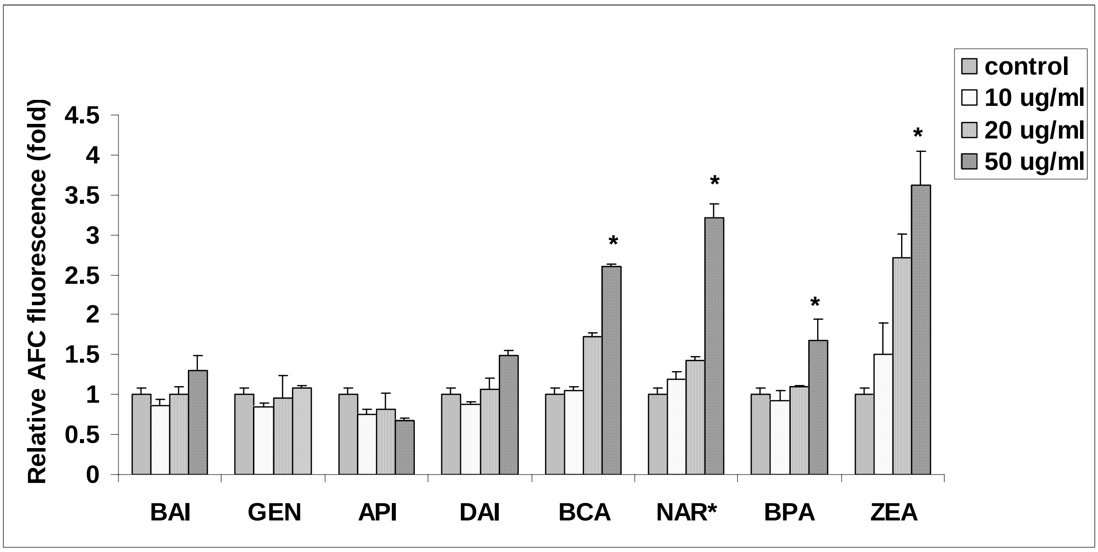

Fig. 9 Caspase-3 activity of human leukemic cells treated with each phytoestrogen. (A) U937 cells and (B) HL-60 cells were treated with individual phytoestrogen for 4 h and fluorogenic peptide substrate DEVD-AMC were added in reaction buffer as indicated in the materials and methods. The increase of fluorescence intensity was compared to control (without treatment) in fold. BAI: baicalein, GEN: genistein, API: apigenin, DAI: daidzein, BCA: biochannin A, NAR: naringenin, BPA: bisphenol A, and ZEA: zearalenone. NAR* concentrations of NAR in both cell treatment increase as 50, 100, 250 µg/ml. ZEA** concentrations of ZEA in U937 cell treatment are in 10, 20, 50 µM. * significantly different compared to control, $p<0.05$.

The mitochondrial transmembrane potential (MTP) was reduced in both HL-60 and U937 apoptotic cells, indicating the involvement of mitochondria. Percent cells with reduced MTP were increased in a dose dependent manner in both leukemic cells (Fig. 10A). This led us to further determine the cytochrome c release from intermembranous space of treated cells' mitochondria. Cytochrome c was released from intermembranous space of mitochondria into cytosol in a dose response pattern (Fig. 10B).

The mitochondrial apoptotic signaling pathway involves activation of the proapoptotic Bcl-2 family member Bax, which induces permeabilization of the mitochondrial outer membrane and release of cytochrome c (85-87). Bax expression was upregulated in time dependent manner as shown in Fig. 10C. The expression of Bcl-2 (anti-apoptotic protein) did not change, whereas Bcl-xL expression was downregulated time-dependently. ZEA induced HL-60 cell apoptosis via increased pro-apoptotic Bax expression and reduced expression of Bcl-xL (anti-apoptotic protein). The increased ratio of Bax/Bcl-xL was observed (Fig. 10D).

A.

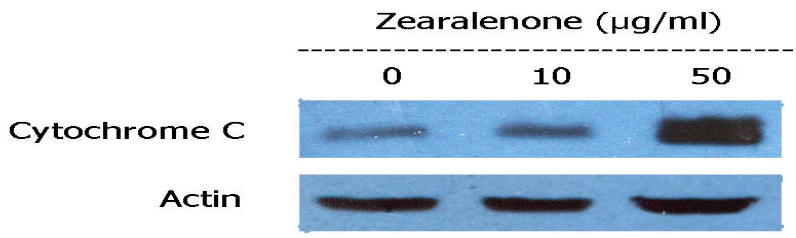

B.

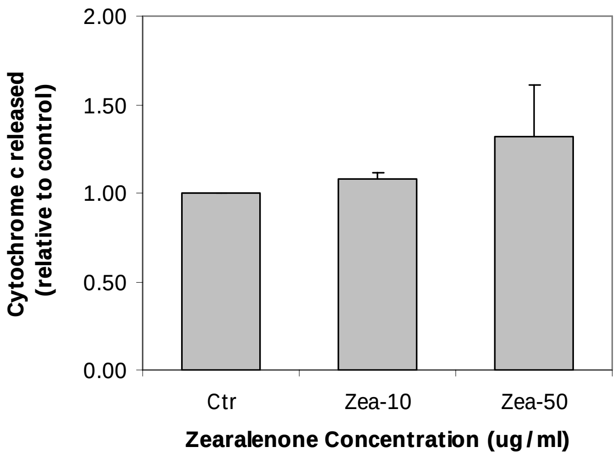

C.

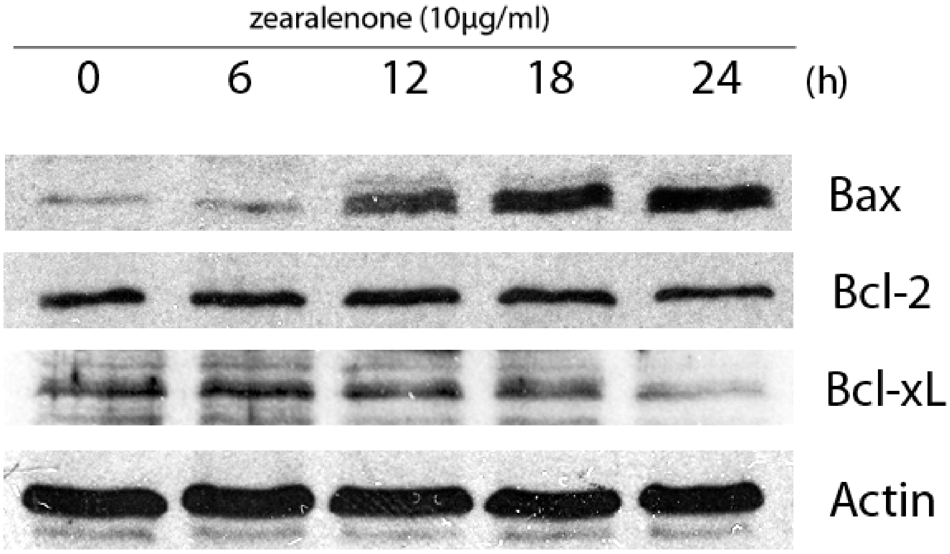

D.

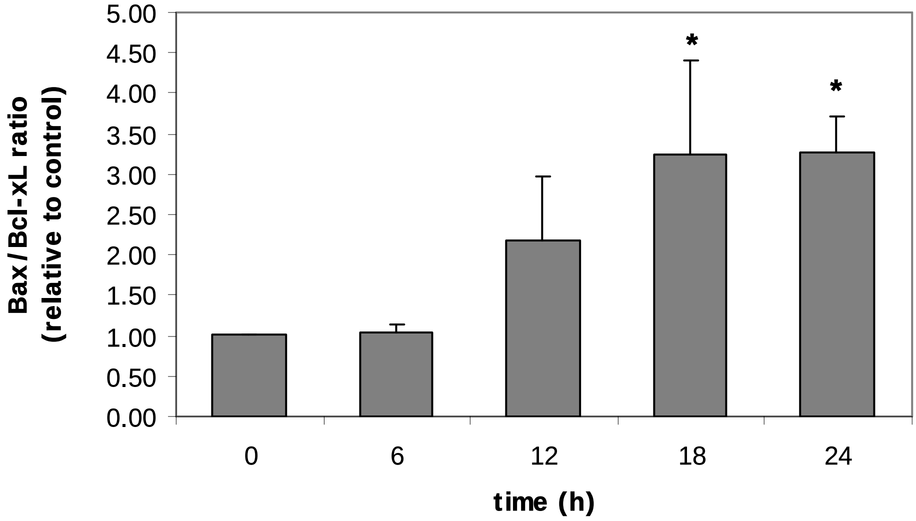

Fig. 10 Release of cytochrome c from mitochondria and the expressions of Bax, Bcl-2 and Bcl-xL in the ZEA-treated HL-60 cells. HL-60 cells were treated with ZEA (10, 50 µg/ml) for 4 h and cytosolic cytochrome c was detected by Western blotting (A). The representative data from three independent experiments are shown (B). Bax, Bcl-2 and Bcl-xL expression (D) and the ratio of Bax/Bcl-xL (E) was from the same sample of cells. The density of bands are plotted as ratio of Bax/Bcl-xL and the results are mean $\pm$ S.E.M. from three independent experiments. *, $p < 0.05$, compared to control.

In apoptotic cells, the proteomics of cholangiocarcinoma cells induced by pomiferin are different from 2 D gel of healthy cholangiocarcinoma cells (88). On comparison between control U937 cells at 4, 24 h and ZEA-treated cells at 4 and 24 h, there were 4 spots of differences as shown in Fig. 11a, including 3 proteins, i.e., (1) fructose bisphosphate aldolase A, muscle type, lung cancer antigen NY LU 1 (arrow 1), (2) glyceraldehydes 3-phosphate dehydrogenase isozymes (arrows 2 and 3) (3) deoxyuridine triphosphate nucleotidohydrolase mitochondrial precursor dUTP pyrophosphatase (arrow 4). GAPDH was an enzyme that activates transcription. The OCA-S transcriptional coactivator complex contains GAPDH and lactate dehydrogenase, two proteins only thought to be involved in metabolism. GAPDH moves between the cytosol and the nucleus and may link the metabolic state to gene transcription. GAPDH initiates apoptosis. GAPDH is S-nitrosylated by NO in response to cell stress, which causes it to bind to the protein Siah1, a ubiquitin ligase. The complex moves into the nucleus where Siah1 targets nuclear protein for degradation, thus initiating controlled cell shutdown (89)

.

There were 23 proteins of different expression in the plasma membrane two-dimensional gel electrophoresis of 24 h ZEA-treated HL-60 cells compared to control (Fig. 11b and Table 2). The upregulated expression of proteins included of 78 kDa glucose-regulated protein or GRP78 (dot no. 3), calreticulin precursor (dot no. 5), endoplasmic reticulum protein ERp29 (dot no. 21), and apoptosis inducing factor (AIF, dot no. 11) in Fig. 11b. The expression of heat shock protein 90 (HSP90) decreased (dot no. 2) functioning for protein folding in ER as shown in Fig. 11b. ZEA used GRP78, calreticulin and ERp29 as transducers to undergo apoptosis through ER stress pathway.

a.

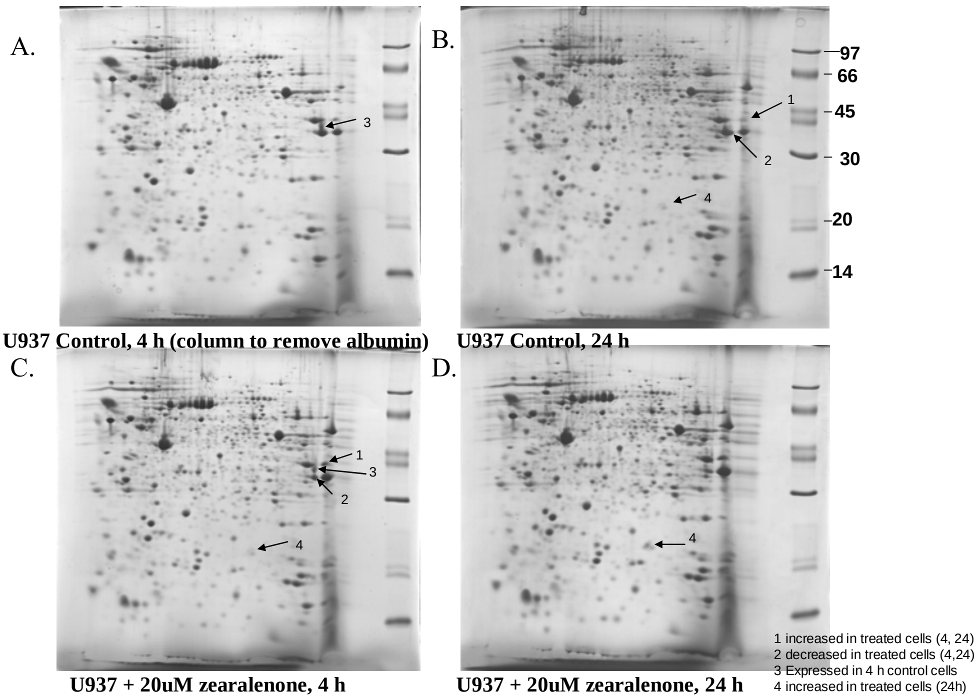

b.

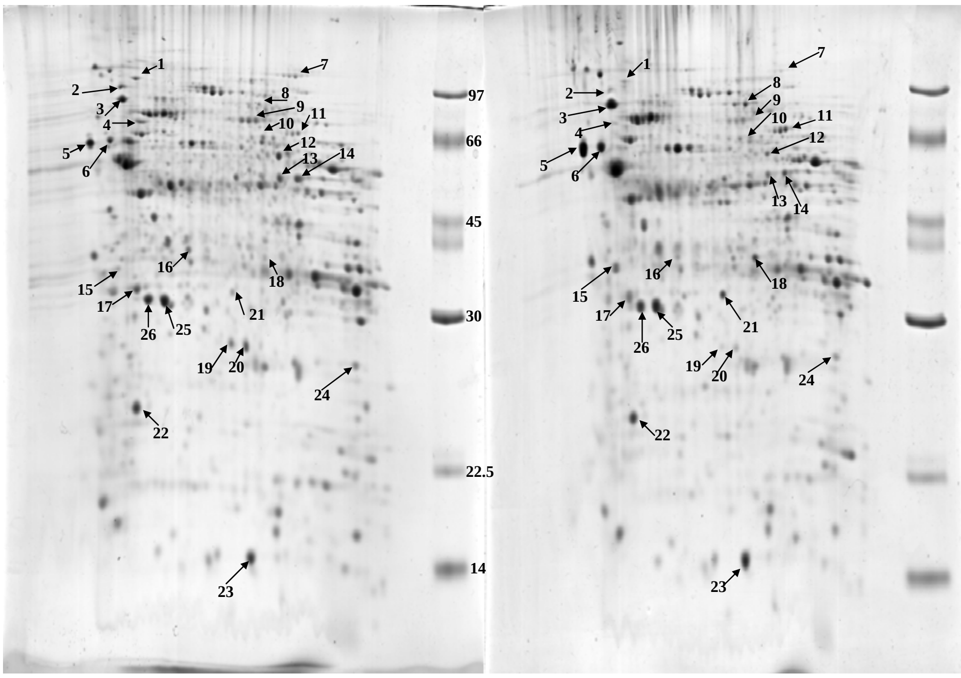

HL-60 Control, Membrane, 24h

HL-60 + Zearalenone, Membrane, 24h

Fig. 11 Two dimensional polyacrylamide gel electrophoresis pattern of U937 and HL-60 cells. U937 cells were cultured for 4 and 24 h in the presence or absence of zearalenone (a). Control 4 h (A), control 24 h (B), cells treated with 20 μM ZEA for 4 h (C) and cells treated with 20 μM ZEA for 24 h (D). There were 4 proteins of differences: Fructose bisphosphate aldolase A, muscle type, lung cancer antigen NY LU1 (arrow 1); glyceraldehyde 3-phosphate dehydrogenase (arrow 2 and 3) and deoxyuridine triphosphate nucleotidohydrolase, mitochondrial precursor (arrow 4). HL-60 cells were cultured for 24 h (b) with (right panel) and without ZEA (left panel). There were 23 protein dots of different expression on plasma membrane. The name list of proteins identified by LC/MS/MS is shown in Table 2.

The involvement of ER is questionable and led us to investigate the ER stress protein, calreticulin (CRT). CRT is an ER-resident stress-regulated chaperone with C-terminal KDEL signal. ER regulates posttranslational protein processing and transport. Under certain circumstances, ER dysfunction leads to the accumulation of unfolded or misfolded proteins in the ER lumen and activates compensatory mechanism, which has been referred to as ER stress response or unfolded protein responses (UPR) (90). Several ER transmembrane proteins are identified as sensors of ER stress. These include pancreatic ER kinase (PERK), inositol requiring enzyme 1 (IRE1) and activating transcription factor 6 (ATF6). PERK phosphorylates the alpha subunit of eukaryotic initiation factor 2 (eIF2alpha), which attenuates the initiation of translation in response to ER stress. The activation of IRE1 and ATF6 signaling promotes pro-apoptotic transcription factor CHOP and the expression of ER-localized chaperones, such as calreticulin, GRP78 and GRP94, which facilitate the restoration of proper protein folding within the ER (90). These protective responses result in an overall decrease in translation, enhanced protein degradation and increased levels of ER chaperones, which consequently increase the protein folding capacity of the ER. However, sustained ER stress ultimately leads to cell death (90). ER stress protein, calreticulin, did not translocate to the cell membrane of human leukemic cells treated with ZEA. ER also regulates calcium ion homeostasis and Ca^{2+} increased in cytosolic and mitochondria, indicating some degree of involvement of ER stress in ZEA-treated human leukemic cells.

The increases in cytosolic and mitochondrial Ca^{2+} levels were found in ER stress (91). Apoptosis induced by ZEA might involve ER stress, so we determine the Ca^{2+} levels in both mitochondria and cytosol. Fig. 12A shows FACS analysis histograms of Fluo3-AM-stained HL-60 cells treated with ZEA at 10 and 20 μg/ml.. Black line represents control, whereas red line represents ZEA-induced cells. Fluo3-stained cells indicated the increase in cytosolic Ca^{2+} level. Rhod2 implied the increase in mitochondrial Ca^{2+} level in ZEA treated cells at 10 and 20 μg/ml (Fig. 12B).

Reduction of endoplasmic reticulum Ca^{2+} levels (ER stress) favors plasma membrane surface exposure of calreticulin (92). When ZEA (10, 20 and 50 μg/ml) was added to the cells and incubated for 30 min, no increase in the expression of calreticulin (CRT) could be detected on the cell membrane of HL-60 cells (Fig. 13).

The cross-talk exists between the two main apoptotic pathways (93, 94). This led us to investigate for the caspase-8 activity in phytoestrogen-induced apoptosis. It was found that caspase-8 activity was increased in BPA-, DAI- and API-induced U937 cell apoptosis and in API-, NAR-, BAI-, ZEA- and DAI-induced HL-60 cell apoptosis as shown in Fig. 14A and 14B. Caspase-8 activity was activated at 24 h of incubation with ZEA in a time dependent manner (Fig. 14C), indicating the death receptor pathway involvement. Caspase-3, an effector caspase, also was activated (Fig. 9). Thus, it means that ZEA-induced human leukemic cell apoptosis involved both intrinsic and extrinsic pathways. It was reported that truncated bid was the linker between the two pathways (95).

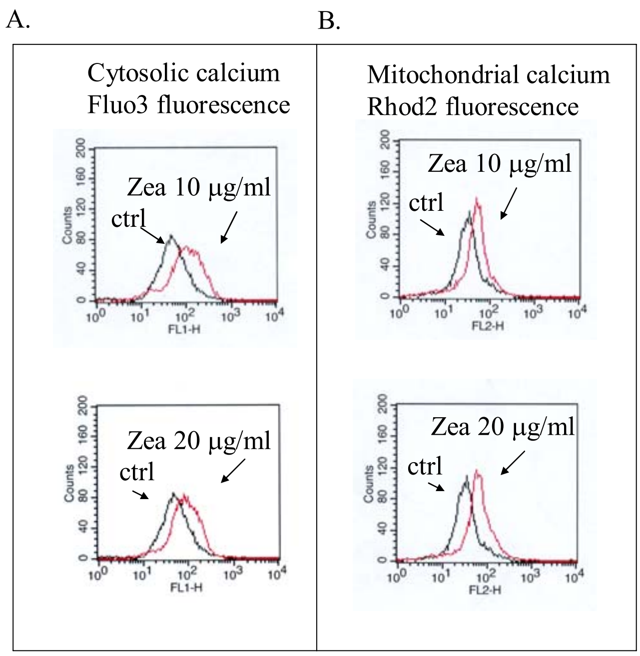

Fig. 12 The enhanced effect of ZEA on cytosolic and mitochondrial Ca^{2+} levels in HL-60 cells. HL-60 cells were incubated with Fluo3 (cytosolic) or Rhod2 (mitochondrial) for 15 min after treatment with and without ZEA for 1 h, then subjected to flow cytometer to detect cytosolic (A) and mitochondrial (B) Ca^{2+} levels as described in Materials and methods. Black trace, control cells; red trace, ZEA-treated cells. The histogram of FACS analysis represents one of three independent experiments.

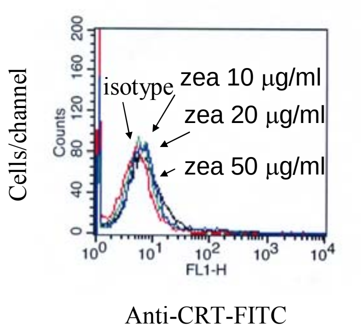

Fig. 13 Cell membrane exposure of calreticulin of ZEA-treated human leukemic cells. HL-60 cells were treated for 30 min with ZEA at indicated concentrations and analyzed for the caltreticulin exposure by flow cytometry. The histogram of FACS analysis represents one of three independent experiments.

A.

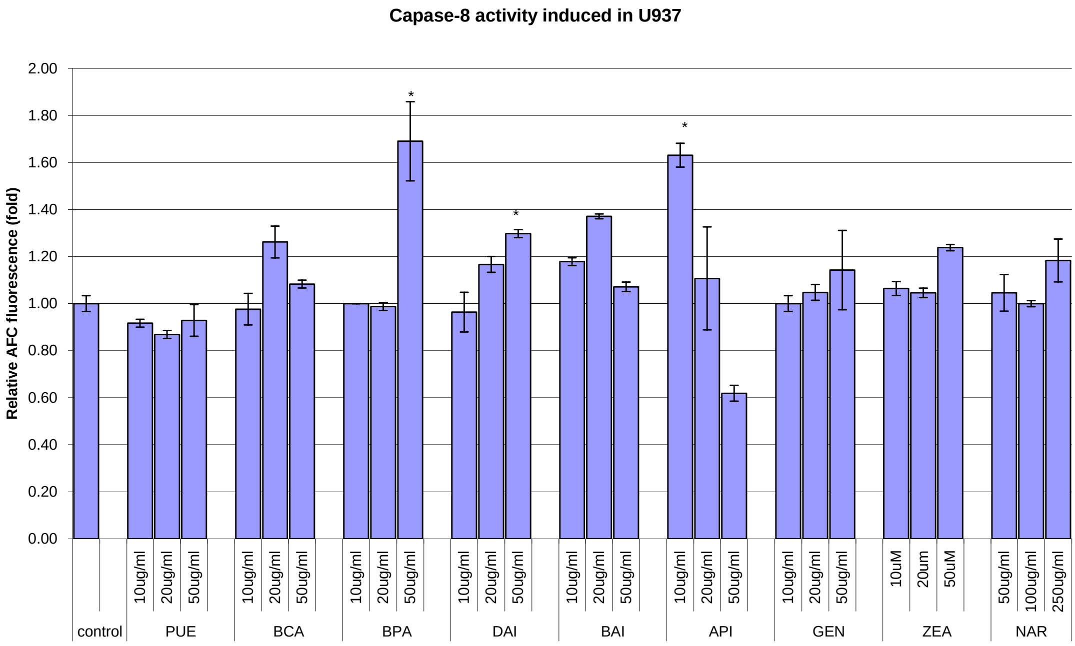

B.

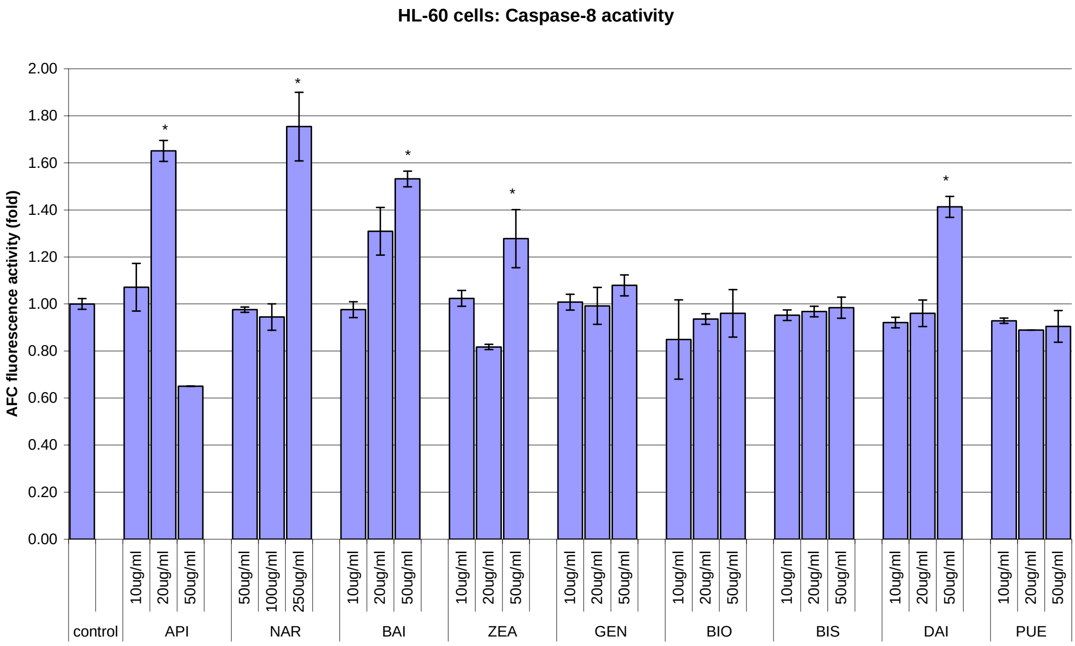

C.

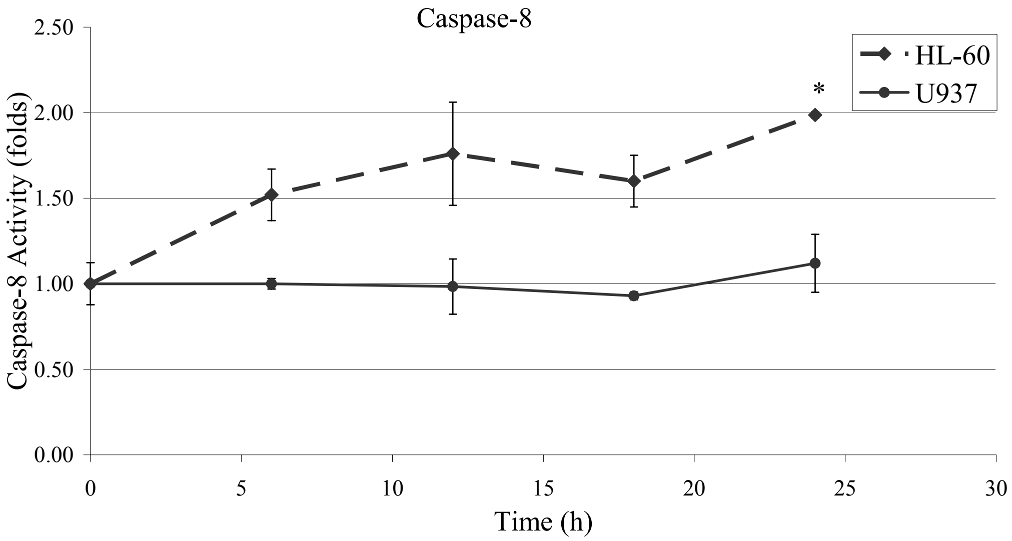

Fig. 14 Effects of phytoestrogens on activation of caspase-8. The activity of caspase-8 in U937 (A) and HL-60 cells (B) at various concentrations of phytoestrogens treated for 4 h were measured using substrate analogs as in Materials and methods. Caspase-8 activity at indicated times (C) was determined by treating HL-60 and U937 cells with ZEA 10 μg/ml and 10 μM, respectively. Data represent mean values ± S.E.M. from three independent experiments. *, $p < 0.05$, compared to control of each type of cells.

Phosphatidylinositol 3-kinase (PI3-K), a group of heterodimeric lipid kinases, functions as a cell survival factor whereas mitogen activated protein kinases (MAPKs) modulate cell proliferation, apoptosis and other biological activities. It is reported that ERK/MAPKs are involved in penta-acetyl geniposide-induced apoptosis via transcription regulation of AP-1 and NF-kappaB (96). PI3-K inhibitor had synergistically effect upon ZEA-treated human leukemic cell apoptosis (Fig. 15). Meanwhile MEK inhibitor (PD98059) increased the percentage of human leukemic U937 cells with reduced MTP when treated with ZEA dose-dependently (Fig 16).

Vinblastine, a chemotherapeutic drug using for treatment of breast cancer and leukemia, when treated in combination with ZEA induced synergistic effect on human leukemic HL-60 cell apoptosis (Fig. 17). This implied the beneficial usage of combined therapy of ZEA and vinblastine in human leukemia.

The effect of PI3-K/MEK inhibitors on human leukemic cells was shown to be synergistic, implying the clinical benefit in combined treatement with ZEA in leukemic patients. This effect was also observed in vinblastine and ZEA, which will reduce the dosage of chemotherapeutic drug and decrease the side effects of the drug but give high efficacy in treatment of leukemic patients.

A.

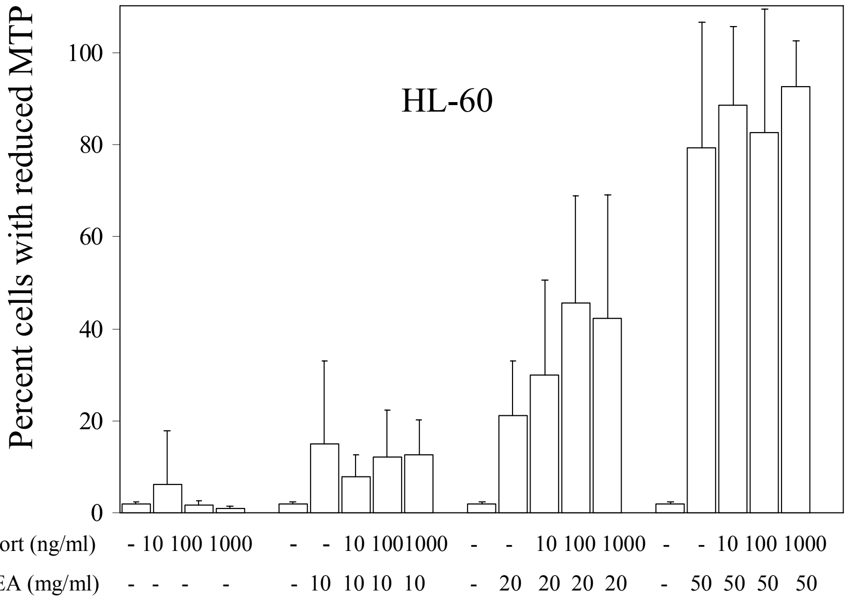

B.

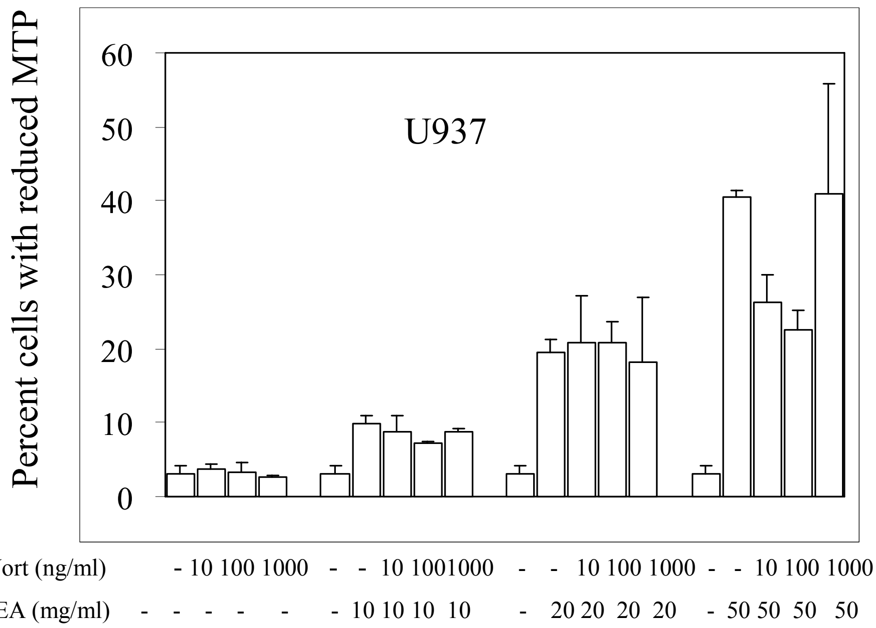

Fig. 15 The effect of PI3-K inhibitor (wortmannin) on the mitochondrial transmembrane potential of ZEA-induced human leukemic HL-60 and U937 cell apoptosis. HL-60 cells (A) and U937 cells (B) were pretreated with wortmannin and then treated with ZEA for 24 h, stained with $DiOC_6$ and analyzed by flow cytometer.

A.

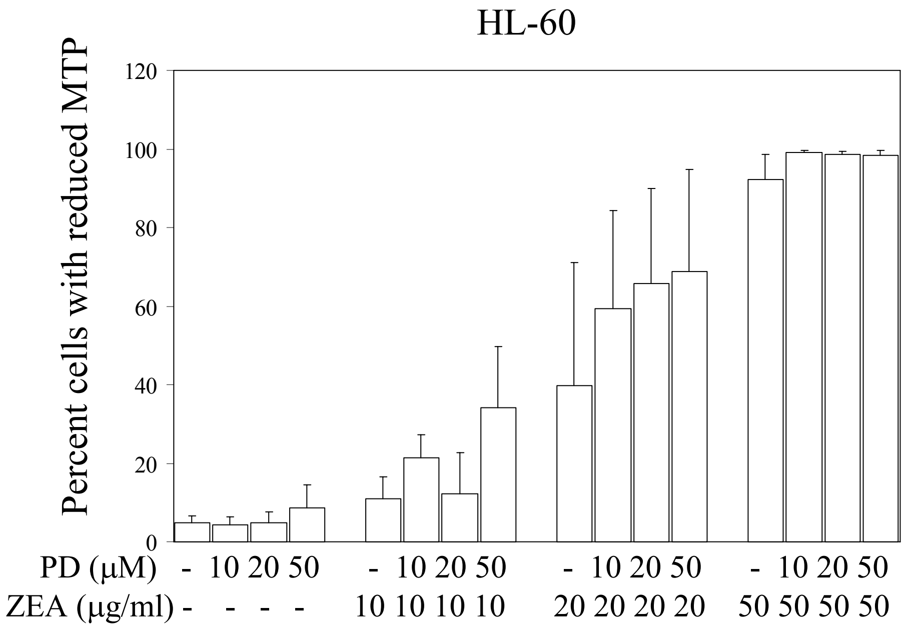

B.

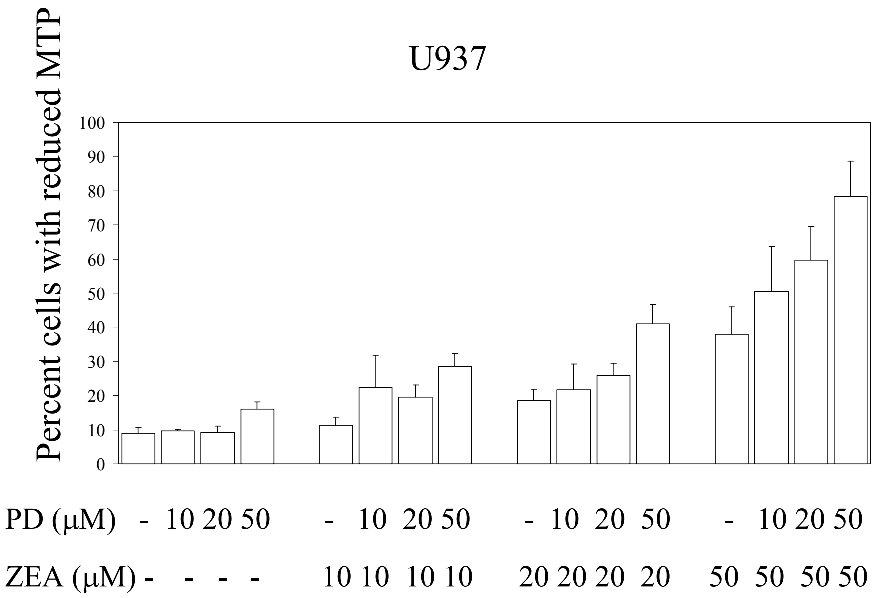

Fig. 16 The effect of ERK/MEK inhibitor (PD98059) on ZEA-induced human leukemic HL-60 and U937 cell apoptosis. HL-60 (A) and U937 cells were pretreated with PD98059 and then treated with ZEA, stained with DiOC6 and processed by flow cytometer. The cells with reduced mitochondrial transmembrane potential were analyzed.

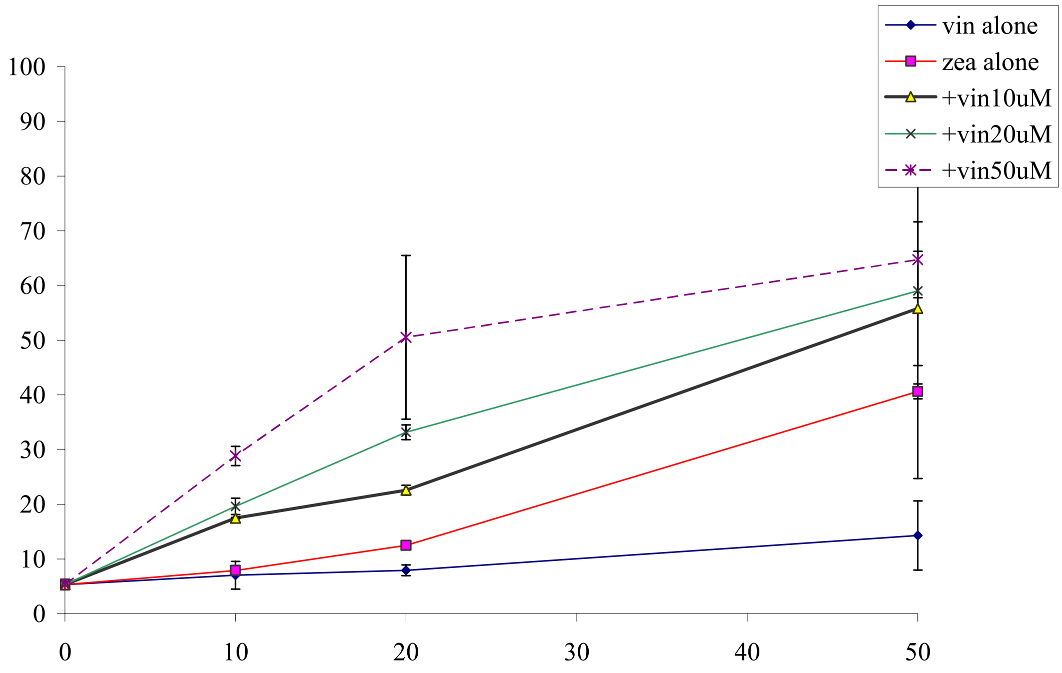

Fig. 17 The synergistic effect of vinblastine on ZEA-induced human promyelocytic leukemic HL-60 cell apoptosis.

CONCLUSION

Nine phytoestrogens are cytotoxic to the human leukemic HL-60 and U937 cell lines except DAI and PUE. Each phytoestrogen caused a reduction of mitochondrial transmembrane potential significantly in both cell lines. They also induced ROS production and cell cycle arrest at specific phase depending on the types and dosages of phytoestrogens and types of cell lines. The phytoestrogen-treated U937 cells showed a dose response in caspase-3 activity significantly including BAI, BCA, NAR, BPA and ZEA. Similar phenomena occurred in phytoestrogen-treated HL-60 cells, viz. BCA, NAR, BPA and ZEA. However, ZEA was selected to study for the molecular mechanism in details. ZEA induced Bax overexpression and Bcl-xL suppression. Cytochrome c release was found in ZEA-induced apoptosis. The 2 D gel electrophoresis showed 3 proteins of different expression in ZEA treated U937 cell, i.e. enzymes in glycolysis and nucleotide pathways and 23 proteins in HL-60 cell membrane included ER stress proteins, viz. CRT, GRP-78, ERp29 and AIF. The cysolic Ca^{2+} and mitochondrial Ca^{2+} levels were increased confirming the ER stress involvement. ZEA caused HL-60 and U937 cell apoptosis via the PI3-K pathway as shown by the synergism of ZEA and PI3-K inhibitor (wortmannin). ERK/MEK inhibitor enhanced the apoptotic effect of ZEA-induced apoptosis in both cell lines. Vinblastine and ZEA also produced synergistic effect on human leukemic HL-60 and U937 cell apoptosis.

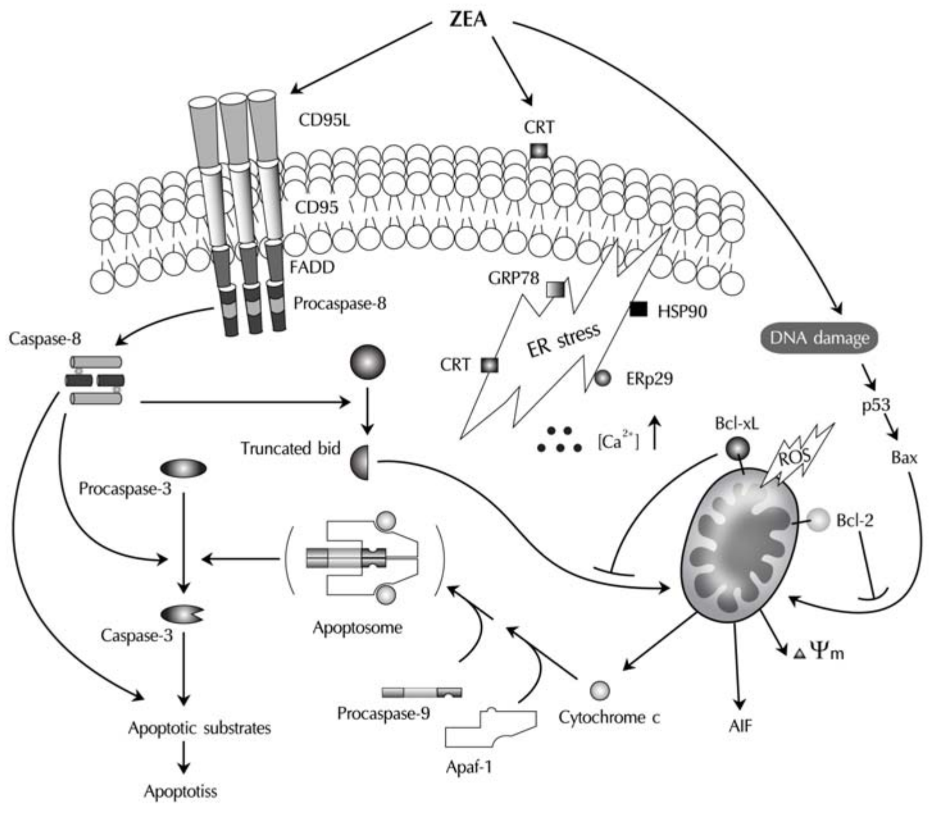

Fig. 18 The proposed mechanism of ZEA-induced human leukemic cell apoptosis.

Table 2 Identified protein spots of HL-60 cells treated with ZEA for 24 h by LC/MS/MS

Spot no.	Protein Name(s)	Description	MW/ pI	Peptide match	% Coverage	Sequence	Expression in treated cells
1	TERA_HUMAN	Transitional endoplasmic reticulum ATPase	89.3/5.18	-	-	-	-1.99
2	GFAP_HUMAN	Glial fibrillary acidic protein	49.8/5.25	1	2.55	(K)LALDIEIATYR(K)	-1.55
	K2C8_HUMAN	Keratin, type II cytoskeletal 8	53.7/5.34	1	2.28		
	HS90A_HUMAN	Heat shock protein HSP 90-alpha	83.2/4.97	7	10.00	K.IDIIPNPQER.T K.EDQTEYLEER.R K.HFSVEGQLEFR.A R.RAPFDLFENK.K R.GVVDSEDLPLNISR.E K.FYEAFSK.N K.EGLELPEDEEEK.K	
3	GRP78_HUMAN	78kDa glucose-regulated protein precursor (GRP 78)	72.3/5.10	-	-	-	1.93
4	PLSL_HUMAN	L-plastin, Lymphocyte cytosolic protein 1	70.2/5.02	11	22.01	(K)AACLPLPGYR(V) (K)IGLFADIELSR(N) (R)NEALIALLR(E) (K)LSPEELLLR(W) (K)AYYHLLEQVAPK(G) (R)QFVTATDVVR(G) (K)LNLAFIANLFNR(Y) (R)VNHLYSDLSDALVIFQLYEK(I) (K)FSLVGIGGQDLNEGNR(T) (R)YTLNILEEIGGGQK(V) (K)VNDDIIVNWVNETLR(E)	-3.1
5	CALR_HUMAN	Calreticulin precursor	60.6/4.37	-	-	-	2.39
6	PDIA1_HUMAN	Protein disulfide isomerase precursor	51.1/4.78	-	-	-	2.86
7	EF2_HUMAN	Elongation factor 2	95.1/6.78	-	-	-	-2.87
8	gi|28317	unnamed protein product	59.5/5.17	3	6.00	R.ALEESNYELEGK.I R.QSVEADINGLR.R	2.26

						R.NVQALEIELQSQLALK.Q	
9	DHSA_HUMAN	Succinate dehydrogenase [ubiquinone] flavoprotein subunit, mitochondrial	72.6/7.04	4	8.43	(R)AAFGLSEAGFNTACVTK(L) (R)GVIALCIEDGSIHR(I) (K)NTVVATGGYGR(T) (R)LGANSLLDLVVFGR(A)	-1.29
	TCPG_HUMAN	T-complex protein 1 subunit gamma	60.5/6.06	1	2.02	(K)TAVETAVLLLR(I)	
10	SERA_HUMAN	D-3-phosphoglycerate dehydrogenase	56.6/6.28	1	2.44	(K)GTIQVITQGTSLK(N)	-1.34
	TCPZ_HUMAN	T-complex protein 1 subunit zeta	58.0/6.22	1	2.26	(K)GIDPFSLDALSK(E)	
	gi|4502643	chaperonin containing TCP1, subunit 6A isoform a	58.0/6.23	7	15.00	R.AQAALAVNISAAR.G K.QADLYISEGLHPR.I R.IITEGFEAAK.E K.ALQFLEEVK.V K.SETDTSLIR.G K.GIDPFSLDALSK.E K.VLAQNSGFDLQETLVK.I	
	gi|1002923	coronin-like protein	51.0/6.12	7	15.00	R.HVFGQPAK.A R.EPVVTLEGHTK.R R.AVFVSEGK.I K.ILTTGFSR.M R.DAGPLLISLK.D R.AAPEASGTPSSDAVSR.L K.LQATVQELQK.R	
11	119623333	apoptosis inducing factor like isoform CRA d Homo sapiens	63.7/10.23	1	1.21	(R)LLSATSR(T)	2.18
	RN112_HUMAN	RING finger protein 112	68.3/8.45	1	1.11	(R)LSGRYPK(V)	
	gi|4557014	catalase [Homo sapiens]	59.7/6.90	12	28.00	K.ADVLTTGAGNPVGDK.L K.LNVITVGPR.G K.GAGAFGYFEVTHDITK.Y R.FR.DPILFPSFIHSQK.R STVAGESGSADTVR.D K.NLSVEDAAR.L R.LSQEDPDYGIR.D R.DLFNAIATGK.Y R.LFAYPDTHR.H	

						K.DAQIFIQK.K K.NFTEVHPDYGSHIQALLDK. Y K.NAIHTFVQSGSHLAAR.E	
	gi|28317	unnamed protein product	59.5/5.17	7	14.00	R.ALEESNYELEGK.I K.YENEVALR.Q R.QSVEADINGLR.R K.ADLEMQIESLTEELAYLK.K R.NVQALEIELQSQLALK.Q K.QSLEASLAETEGR.Y R.LENEIQTYR.S	
12	SAM50_HUMAN	Sorting and assembly machinery component 50 homolog	51.9/6.46	5	14.50	(K)VNQELAGYTGGDVSFIK(E) (K)EDFELQLNK(Q) (R)THFFLNAGNLCNLNYGEGP K(A) (R)WSYGAGIVLR(L) (R)ICDGVQFGAGIR(F)	-1.98
	gi|7022134	unnamed protein product	51.9/6.62	9	20.00	K.DVVVQHVHFDGLGR.T K.VTFQFSYGTK.E R.NFSVNLYK.V K.VTGQFPWSSLR.E K.WEGVWR.E K.VNQELAGYTGGDVSFIK.E K.EDFELQLNK.Q R.FYLGGPTSVR.G R.WSYGAGIVLR.L	
	gi|4929571	CGI-51 protein	52.1/6.85	10	26.00	K.DVVVQHVHFDGLGR.T K.VTFQFSYGTK.E R.NFSVNLYK.V K.VTGQFPWSSLR.E K.WEGVWR.E K.VNQELAGYTGGDVSFIK.E K.EDFELQLNK.Q K.QLIFDSVFSASFWGGMLVPI GDKPSSIADRFYLGGPTSIR.G	

						R.FYLGGPTSIR.G R.WSYGAGIVLR.L	
	ANX11_HUMAN	Annexin A11	54.3/7.53	5	11.00	R.GTITDAPGFDPLR.D K.TPVLFDIYEIK.E R.LLISLSQGNR.D R.SETDLLDIR.S K.SLYHDISGDTSGDYR.K	
13,14	ENOA_HUMAN	Alpha-enolase	47.0/7.54	-	-	-	-1.57, -1.88
15	119571303	spectrin domain with coiled coils 1 isoform CRA d Homo sapiens	28.9/4.97	1	4.20	(R)LQIVSLASWAR(A)	5.14
	ATPG_HUMAN	ATP synthase subunit gamma, mitochondrial	33.0/9.56	1	4.03	(R)IYGLGSLALYEK(A)	
	TPM3_HUMAN	Tropomyosin alpha-3 chain	32.8/4.49	1	2.82	(K)HIAEEADR(K)	
	ES8L1_HUMAN	Epidermal growth factor receptor kinase substrate 8-like protein 1	80.3/5.66	1	0.69	(K)SGPSR(K)	
	gi|16877071	ATP synthase, H+ transporting, mitochondrial F1 complex, gamma polypeptide 1	32.9/9.23	3	11.00	R.IYGLGSLALYEK.A K.HLLIGVSSDR.G K.ELIEIISGAAALD.-	
16	LDHB_HUMAN	L-lactate dehydrogenase B chain	36.6/5.64	2	8.08	(K)SLADELALVDVLEDK(L) (R)VIGSGCNLDSAR(F)	-1.62
	AFF4_HUMAN	AF4/FMR2 family member 4	12.7/9.68	1	0.77	(K)NSSSTSKQK(K)	
17	COMT_HUMAN	Catechol O-methyltransferase	30.0/5.12	2	14.02	(K)VTLVVGASQDIIPQLK(K) (K)GTVLLADNVICPGAPDFLA HVR(G)	1.07
	PODXL_HUMAN	Podocalyxin like protein 1 precursor	55.6/5.23	1	2.46	(R)LASVPGSQTVVVK(E)	
	121944562	immunoglobulin A heavy chain variable region Homo sapiens	11.9/5.64	1	5.50	(K)VDGIEK(Y)	
	TRM13_HUMAN	tRNA guanosine-2'-O-methyltransferase TRM13 homolog	54.2/8.01	1	2.49	(R)KTSLETSNSTTK(R)	
18	ANXA1_HUMAN	Annexin A1	38.7/6.63	5	22.00	K.GGPGSAVSPYPTFNPSSDVA ALHK.A	3.25

						K.GVDEATIIDILTK.R K.ALTGHLEEVVLALLK.T K.TPAQFDADELR.A K.GTDVNVFNTILTTR.S	
	CN102_HUMAN	UPF0614 protein C14orf102	13.2/7.60	1	0.52	(R)LISLAK(C)	
19	SOCS4_HUMAN	Suppressor of cytokine signaling 4	50.6/6.64	1	1.36	(R)SDLAFR(W)	-3.12
	K2C1_HUMAN	Keratin, type II cytoskeletal 1(CK-1)	65.8/8.16	4	5.00	R.QFSSR.S K.AEAESLYQSK.Y K.YEELQITAGR.H K.LALDLEIATYR.T	
	K2C7_HUMAN	Keratin, type II cytoskeletal 7 (CK-7)	51.2/5.50	1	2.00	K.LALDIEIATYR.K	
20	gi|189054178	unnamed protein product [Homo sapiens]	66.0/7.62	4	6.00	R.SLDLDSIIAEVK.A K.YEELQITAGR.H K.LNDLEDALQQAK.E R.TLLEGEESR.M	-2.84
21	AF047368_1	nebulette Homo sapiens	11.6/7.98	1	0.99	(K)ENQGNISSVK(Y)	2.99
	ERP29_HUMAN	Endoplasmic reticulum protein ERp29	29.0/6.77	7	22.00	K.GALPLDTVTFYK.V K.GALPLDTVTFYK.V K.FVLVK.F R.DGDFENPVPYTGAVK.V K.QGQDNLSSVK.E K.WAEQYLK.I K.SLNILTAFQK.K	
22	ATP5H_HUMAN	ATP synthase subunit d, mitochondrial	18.5/5.21	6	40.00	K.TIDWVAFAEIIPQNQK.A K.SWNETLTSR.L R.LAALPENPPAIDWAYYK.A K.AGLVDDFEK.K K.YTAQVDAEEK.E K.YTAQVDAEEKEDVK.S	-1.08
	gi|189054178	unnamed protein product	66.0/7.62	3	5.00	K.SLNNQFASFIDK.V R.SLDLDSIIAEVK.A K.LALDLEIATYR.T	
23	B2MG_HUMAN	Beta-2 microglobulin	12.7/5.77	2	18.00	R.VNHVTLSQPK.I K.VEHSDLSFSK.D	1.35

24	NDUBA_HUMAN	NADH dehydrogenase [ubiquinone] 1 beta subcomplex subunit 10	20.8/8.60	3	20.35	(K)AFDLIVDRPVTLVR(E) (K)EVEQFTQVAK(A) (R)YQDLGAYSSAR(K)	-1.05
	gi|189054178	unnamed protein product	65.9/7.62	7	12.00	R.TNAENEFVTIK.K R.SLDLDSIIAEVK.A K.YEELQITAGR.H K.LNDLEDALQQAK.E K.LALDLEIATYR.T R.TLLEGEESR.M R.GSGGGSSGGSIGGR.G	
25	ASCC1_HUMAN	Activating signal cointegrator 1 complex subunit 1	45.48/5.22	1	1.75	(R)SFALLPR(L)	1.11
	PHB_HUMAN	prohibitin	29.8/5.57	11	52.00	K.FGLALAVAGGVVNSALYNV DAGHR.A K.DLQNVNITLR.I R.FDAGELITQR.E R.AATFGLILDDVSLTHLTFGK.E K.EFTEAVEAK.Q K.QVAQQEAER.A K.AAIISAEGDSK.A K.AAELIANSLATAGDGLIELR.K R.KLEAAEDIAYQLSR.S K.LEAAEDIAYQLSR.S R.NITYLPAGQSVLLQLPQ.-	
26	PHB_HUMAN	Prohibitin	29.8/5.57	13	59.00	K.VFESIGK.F K.DLQNVNITLR.I R.ILFRPVASQLPR.I R.IFTSIGEDYDER.V R.VLPSITTEILK.S R.FDAGELITQR.E R.AATFGLILDDVSLTHLTFGK.E K.EFTEAVEAK.Q	1.06

						K.QVAQQEAER.A K.AAIISAEGDSK.A K.AAELIANSLATAGDGLIELR. K R.KLEAAEDIAYQLSR.S R.NITYLPAGQSVLLQLPQ.-	
	NDUS3_HUMAN	NADH dehydrogenase [ubiquinone] iron-sulfur protein 3, mitochondrial	30.2/6.99	2	9.00	K.SLVDLTAVDVPTR.Q K.DFPLSGYVELR.Y	

Note: Spot no. 1, 3, 5, 7, 13 and 14 were matched from our hepatocellular carcinoma cell line database. The density of spots were calculated as percent volume and shown in this table as expression fold.

REFERENCES

1. Lin HY, Shen SC, Lin CW, Yang LY, Chen YC. Baicalein inhibition of hydrogen peroxide-induced apoptosis via ROS-dependent heme oxygenase 1 gene expression. Biochim Biophys Acta. 2007;1773:1073-86.
2. Chen FL, Wang XZ, Li JY, Yu JP, Huang CY, Chen ZX. 12-lipoxygenase induces apoptosis of human gastric cancer AGS cells via the ERK1/2 signal pathway. Dig Dis Sci 2008;53:181-7.
3. Lee SW, Song GS, Kwon CH, Kim YK. Beneficial effect of flavonoid baicalein in cisplatin-induced cell death of human glioma cells. Neurosci Lett. 2005;382:71-5.
4. Sonnenschein C, Soto AM. An updated review of environmental estrogen and androgen mimics and antagonists. J Steroid Biochem Mol Biol 1998;65:143-50.
5. Antignac JP, Cariou R, Le Bizec B, Cravedi JP, Andre F. Identification of phytoestrogens in bovine milk using liquid chromatography/electrospray tandem mass spectrometry. Rapid Commun Mass Spectrom. 2003;17:1256-64.
6. Herbst AL, Green THJ, Ulfelder H. Primary carcinoma of the vagina. An analysis of 68 cases. Am J Obstet Gynecol. 1970;106:210-8.
7. Watson CS, Bulayeva NN, Wozniak AL, Alyea RA. Xenoestrogens are potent activators of nongenomic estrogenic responses. Steroids. 2007;72:124-34.
8. Haighton LA, Hlywka JJ, Doull J, Kroes R, Lynch BS, Munro IC. An evaluation of the possible carcinogenicity of bisphenol A to humans. Regul Toxicol Pharmacol. 2002;35:238-54.
9. Lin Y, Zeng XG, Wu DS, X W. Study on bisphenol A induced primary cultured mesencephalic neuronal cell injury by oxidative stress. Wei Sheng Yan Jiu. 2006;35:419-22.
10. Iida H, Maehara K, Doiguchi M, Mōri T, Yamada F. Bisphenol A-induced apoptosis of cultured rat Sertoli cells. Reprod Toxicol. 2003;17:457-64.
11. Oka T, Adati N, Shinkai T, Sakuma K, Nishimura T, Kurose K. Bisphenol A induces apoptosis in central neural cells during early development of Xenopus laevis. Biochem Biophys Res Commun. 2003;312:877-82.
12. Xu J, Osuga Y, Yano T, Morita Y, Tang X, Fujiwara T, et al. Bisphenol A induces apoptosis and G2-to-M arrest of ovarian granulosa cells. Biochem Biophys Res Commun. 2002;292:456-62.
13. Yu Z, Zhang L, Wu D. Effects of three environmental estrogens on expression of proliferation and apoptosis-associated genes in PEO4 cells. Wei Sheng Yan Jiu. 2004;33:404-6.
14. Yu Z, Zhang L, Wu D. Effects of environmental estrogens on apoptosis induced by estrogen depletion in T47D cells. Zhonghua Yu Fang Yi Xue Za Zhi. 2003;37:395-7.
15. Negishi T, Ishii Y, Kyuwa S, Kuroda Y, Yoshikawa Y. Inhibition of staurosporine-induced neuronal cell death by bisphenol A and nonylphenol in primary cultured rat hippocampal and cortical neurons. Neurosci Lett. 2003;353:99-102.
16. Diel P, Olff S, Schmidt S, Michna H. Effects of the environmental estrogens bisphenol A, o,p'-DDT, p-tert-octylphenol and coumestrol on apoptosis induction, cell proliferation and the expression of estrogen sensitive molecular parameters in the human breast cancer cell line MCF-7. J Steroid Biochem Mol Biol. 2002;80:61-70.
17. Hughes PJ, McLellan H, Lowes DA, Kahn SZ, Bilmen JG, Tovey SC, et al. Estrogenic alkylphenols induce cell death by inhibiting testis endoplasmic reticulum Ca(2+) pumps. Biochem Biophys Res Commun. 2000;277:568-74.

18. Satoh K, Ida Y, Tomioka M, Shiohara K, Sakagami H, Fujisawa S. Interaction between antioxidants and hydroquinone/bisphenol. Anticancer Res. 1999;19:5457-62.
19. Kanno S, Tomizawa A, Ohtake T, Koiwai K, Ujibe M, Ishikawa M. Naringenin-induced apoptosis via activation of NF-kappaB and necrosis involving the loss of ATP in human promyeloleukemia HL-60 cells. Toxicol Lett. 2006;166:131-9.
20. Totta P, Acconcia F, Leone S, Cardillo I, Marino M. Mechanisms of naringenin-induced apoptotic cascade in cancer cells: involvement of estrogen receptor alpha and beta signalling. IUBMB Life. 2004;56:491-9.
21. Janardhana GR, Rabeas KA, Shekar Shetty H. Mycotoxin contamination of maize grains grown in Karnataka (India). Food Chem Toxicol. 1999;37:863-8.
22. Reza Oveisi M, Hajimahmoodi M, Memarian S, Sadeghi N, Shoeibi S. Determination of zearalenone in corn flour and a cheese snack product using high-performance liquid chromatography with fluorescence detection. Food Addit Contam. 2005;22:443-8.
23. Minervini F, Giannoccaro A, Cavallini A, Visconti A. Investigations on cellular proliferation induced by zearalenone and its derivatives in relation to the estrogenic parameters. Toxicol Lett. 2005;159:272-83.
24. D'Mello JPF, Placinta CM, MacDonald AMC. Fusarium mycotoxins: a review of global animal health, welfare and reproductivity. Anim Feed Sci Technol. 1999;78:183-205.
25. Minervini F, Dell'Aquila ME, Maritato F, Minoia P, Visconti A. Toxic effects of the mycotoxin zearalenone and its derivatives on in vitro maturation of bovine oocytes and 17[beta]-estradiol levels in mural granulosa cell cultures. Toxicol In Vitro. 2001;15:489-95.
26. Placinta CM, D'Mello, J. P. F., MacDonal, A. M. C. A review of worldwide contamination of cereal grains and animal feed with Fusarium mycotoxins. Anim Feed Sci Technol. 1999;78:21-37.
27. Lioi MB, Santoro A, Barbieri R, Salzano S, Ursini MV. Ochratoxin A and zearalenone: a comparative study on genotoxic effects and cell death induced in bovine lymphocytes. Mutat Res. 2004;557:19-27.
28. Ouanes Z, Sbid S, Ayed I, Anane R, Mobio T, Creppy EE, et al. Induction of micronuclei by zearalenone in Vero monkey kidney cells and in bone marrow cells of mice: protective effect of vitamin E. Mutat Res. 2003;538:63-70.
29. Grosse Y, Chekir-Ghedira L, Huc A, Obrecht-Pfumio S, Dirheimer G, Bacha H, et al. Retinol, ascorbic acid and alpha-tocopherol prevent DNA adduct formation in mice treated with the mycotoxins ochratoxin A and zearalenone. Cancer Lett. 1997;114:225-9.
30. Abid-Essefi S, Baudrimont I, Hassen W, Ouanes Z, Mobio TA, Anane R, et al. DNA fragmentation, apoptosis and cell cycle arrest induced by zearalenone in cultured DOK, Vero and Caco-2 cells: prevention by vitamin E. Toxicology. 2003;192:237-48.
31. Kim IH, Son HY, Cho SW, Ha CS, Kang BH. Zearalenone induces male germ cell apoptosis in rats. Toxicol Lett. 2003;138:185-92.
32. Kouadio JH, Mobio TH, Baudrimont I, Moukha S, Dano SD, Creppy EE. Comparative study of cytotoxicity and oxidative stress induced by deoxynivalenol, zearalenone or fumonisin B1 in human intestinal cell line Caco-2. Toxicology. 2005;213:56-65.
33. Cetin Y, Bullerman LB. Cytotoxicity of Fusarium mycotoxins to mammalian cell cultures as determined by the MTT bioassay. Food Chem Toxicol. 2005;43:755-64.

34. Vlata Z, Porichis F, Tzanakakis G, Tsatsakis A, Krambovitis E. A study of zearalenone cytotoxicity on human peripheral blood mononuclear cells. Toxicol Lett. 2006;165:274-81.
35. Ahamed S, Foster JS, Bukovsky A, Wimalasena J. Signal transduction through the Ras/Erk pathway is essential for the mycoestrogen zearalenone-induced cell-cycle progression in MCF-7 cells. Mol Carcinog. 2001;30:88-98.
36. Wang S, DeGroff VL, Clinton SK. Tomato and soy polyphenols reduce insulin-like growth factor-I-stimulated rat prostate cancer cell proliferation and apoptotic resistance in vitro via inhibition of intracellular signaling pathways involving tyrosine kinase. J Nutr. 2003;133:2367-76.
37. Proteggente AR, England TG, Rehman A, Rice-Evans CA, Halliwell B. Gender differences in steady-state levels of oxidative damage to DNA in healthy individuals. Free Radic Res. 2002;36:157-62.
38. Su SJ, Chow NH, Kung ML, Hung TC, Chang KL. Effects of soy isoflavones on apoptosis induction and G2-M arrest in human hepatoma cells involvement of caspase-3 activation, Bcl-2 and Bcl-XL downregulation, and Cdc2 kinase activity. Nutr Cancer. 2003;45:113-23.
39. Tsutsui T, Tamura Y, Yagi E, Someya H, Hori I, Metzler M, et al. Cell-transforming activity and mutagenicity of 5 phytoestrogens in cultured mammalian cells. Int J Cancer. 2003;105:312-20.
40. Jarred RA, Keikha M, Dowling C, McPherson SJ, Clare AM, Husband AJ, et al. Induction of apoptosis in low to moderate-grade human prostate carcinoma by red clover-derived dietary isoflavones. Cancer Epidemiol Biomarkers Prev. 2002;11:1689-96.
41. Azuma Y, Onishi Y, Sato Y, Kizaki H. Effects of protein tyrosine kinase inhibitors with different modes of action on topoisomerase activity and death of IL-2-dependent CTLL-2 cells. J Biochem. 1995;118:312-8.
42. Boersma BJ, Barnes S, Kirk M, Wang CC, Smith M, Kim H, et al. Soy isoflavonoids and cancer -- metabolism at the target site. Mutat Res. 2001;480-481:121-7.
43. Hsu JT, Ying C, Chen CJ. Regulation of inducible nitric oxide synthase by dietary phytoestrogen in MCF-7 human mammary cancer cells. Reprod Nutr Dev. 2000;40:11-8.
44. Balabhadrapathruni S, Thomas TJ, Yurkow EJ, Amenta PS, Thomas T. Effects of genistein and structurally related phytoestrogens on cell cycle kinetics and apoptosis in MDA-MB-468 human breast cancer cells. Oncol Rep. 2000;7:3-12.
45. Su SJ, Yeh TM, Lei HY, Chow NH. The potential of soybean foods as a chemoprevention approach for human urinary tract cancer. Clin Cancer Res. 2000;6:230-6.
46. Zhou JR, Mukherjee P, Gugger ET, Tanaka T, Blackburn GL, Clinton SK. Inhibition of murine bladder tumorigenesis by soy isoflavones via alterations in the cell cycle, apoptosis, and angiogenesis. Cancer Res. 1998;58:5231-8.
47. Yanagihara K, Ito A, Toge T, Numoto M. Antiproliferative effects of isoflavones on human cancer cell lines established from the gastrointestinal tract. Cancer Res. 1993;53:5815-21.
48. Fan LL, Sun LH, Li J, Yue XH, Yu HX, Wang SY. The protective effect of puerarin against myocardial reperfusion injury. Study on cardiac function. Chin Med J. 1992;105:11-7.

49. Xuan B, Zhou YH, Yang RL, Li N, Min ZD, Chiou GC. Improvement of ocular blood flow and retinal functions with puerarin analogs. J Ocul Pharmacol Ther. 1999;15 207-16.
50. Hsu FL, Liu IM, Kuo DH, Chen WC, Su HC, Cheng JT. Antihyperglycemic effect of puerarin in streptozotocin-induced diabetic rats. J Nat Prod. 2003;66:788-92.
51. Xu XH. Effects of puerarin on fatty superoxide in aged mice induced by D-galactose. Zhongguo Zhong Yao Za Zhi. 2003;28:66-9.
52. Chung CS, Jiang Y, Cheng D, Birt DF. Impact of adenomatous polyposis coli (APC) tumor supressor gene in human colon cancer cell lines on cell cycle arrest by apigenin. Mol Carcinog. 2007;46:773-82.
53. Balasubramanian S, Eckert RL. Keratinocyte proliferation, differentiation, and apoptosis--differential mechanisms of regulation by curcumin, EGCG and apigenin. Toxicol Appl Pharmacol. 2007;224:214-9.
54. Laberge RM, Karwatsky J, Lincoln MC, Leimanis ML, Georges E. Modulation of GSH levels in ABCC1 expressing tumor cells triggers apoptosis through oxidative stress. Biochem Pharmacol. 2007;73:1727-37.
55. Watanabe N, Hirayama R, Kubota N. The chemopreventive flavonoid apigenin confers radiosensitizing effect in human tumor cells grown as monolayers and spheroids. J Radiat Res (Tokyo). 2007;48:45-50.
56. Kumazawa Y, Kawaguchi K, Takimoto H. Immunomodulating effects of flavonoids on acute and chronic inflammatory responses caused by tumor necrosis factor alpha. Curr Pharm Des. 2006;12:4271-9.
57. Fang J, Zhou Q, Liu LZ, Xia C, Hu X, Shi X, et al. Apigenin inhibits tumor angiogenesis through decreasing HIF-1alpha and VEGF expression. Carcinogenesis. 2007;28:858-64.
58. Horinaka M, Yoshida T, Shiraishi T, Nakata S, Wakada M, Sakai T. The dietary flavonoid apigenin sensitizes malignant tumor cells to tumor necrosis factor-related apoptosis-inducing ligand. Mol Cancer Ther. 2006;5:945-51.
59. Chiang LC, Ng LT, Lin IC, Kuo PL, Lin CC. Anti-proliferative effect of apigenin and its apoptotic induction in human Hep G2 cells. Cancer Lett. 2006;18:207-14.
60. Liu LZ, Fang J, Zhou Q, Hu X, Shi X, Jiang BH. Apigenin inhibits expression of vascular endothelial growth factor and angiogenesis in human lung cancer cells: implication of chemoprevention of lung cancer. Mol Pharmacol. 2005;68:635-43.
61. Chen D, Daniel KG, Chen MS, Kuhn DJ, Landis-Piwowar KR, Dou QP. Dietary flavonoids as proteasome inhibitors and apoptosis inducers in human leukemia cells. Biochem Pharmacol. 2005;69:1421-32.
62. Dias N, Bailly C. Drugs targeting mitochondrial functions to control tumor cell growth. Biochem Pharmacol. 2005;70:1-12.
63. Schulze-Osthoff K, Ferrari D, Los M, Wesselborg S, Peter M. Apoptosis signaling by death receptors. Eur J Biochem. 1998 254:439-59.
64. Rao RV, Ellerby HM, Bredesen DE. Coupling endoplasmic reticulum stress to the cell death program. Cell Death Differ. 2004;11:372-80.
65. Budihardjo I, Oliver H, Lutter M, Luo X, Wang X. Biochemical pathways of caspase activation during apoptosis. Annu Rev Cell Dev Biol. 1999;15:269-90.
66. Li UX, Kim CN, Yang J, Jemmerson R, Wang X. Induction of apoptotic program in cell-free extracts: requirement for dATP and cytochrome c. Cell. 1996;86:147-57.
67. Thorburn A. Death receptor-induced cell killing. Cell Signal. 2004;16:139-44.

68. Boyce M, Yuan J. Cellular response to endoplasmic reticulum stress: a matter of life or death. Cell Death Differ. 2006;13:363-73.
69. Yamaguchi H, Wang HG. CHOP is involved in endoplasmic reticulum stress-induced apoptosis by enhancing DR5 expression in human carcinoma cells. J Biol Chem. 2004;279:45495-502.
70. Yamaguchi H, Bhalla K, Wang HG. Bax plays a pivotal role in thapsigargin-induced apoptosis in human colon HT116 cells by controlling Smac/Diablo and Omi/HrtA2 release from mitochondria. Cancer Res. 2003;63:1483-9.
71. Johnson S, Michalak M, Opas M, Eggleton P. The ins and outs of calreticulin: from the ER lumen to the extracellular space. Trends Cell Biol. 2001;11:122-9.
72. Michalak M, Corbett EF, Mesaeli N, Nakamura K, Opas M. Calreticulin: one protein, one gene, many functions. Biochem J. 1999;344:281-92.
73. Gardai SJ, McPhillips KA, Frasch SC, Janssen WJ, Starefeldt A, Murphy-Ullrich JE. Cell surface calreticulin initiates clearance of viable or apoptotic cells through transactivation of LRP on the phagocyte. Cell. 2005;123:321-34.
74. Obeid M, Tesniere A, Ghringhelli F, Fimia GM, Apetoh L, Perfettini JL. Calreticulin exposure dictates the immunogenicity of cancer cell death. Nat Med. 2007;13:54-61.
75. Casares N, Pequignot MO, Tesniere A, Ghringhelli F, Roux S, Chaput N. Caspase-dependent immunogenicity of doxorubicin-induced tumor cell death. J Exp Med. 2005;202:1691-701.
76. Apetoh L, Ghringhelli F, Tesniere A, Obeid M, Ortiz C, Criolo A. Toll-like receptor 4-dependent contribution of the immune system to anti-cancer chemo- and radiotherapy. Nat Med. 2007;4:65-70.
77. Srivastava PK. Heat shock protein-based novel immunotherapies. Drug News Perspect. 2000;13:517-22.
78. Su WC, Chang SL, Chen TY, Chen JS, Tsao CJ. Comparison in in vitro growth-inhibitory activity of carboplatin and cisplatin on leukemic cells and hematopoietic progenitors: the myelosuppressive activity of carboplatin may be greater than its antileukemic effect. Jpn J Clin Oncol. 2002;30:562-7.
79. Banjerdpongchai R, Wilairat P. Effects of water-soluble antioxidants and MAPKK/MEK inhibitor on curcumin-induced apoptosis in HL-60 human leukemic cells. Asian Pac J Cancer Prev. 2005;6:282-5.
80. Yoshino M, Haneda M, Naruse M, Htay HH, Tsubouchi R, Qiao SL, et al. Prooxidant activity of curcumin: copper-dependent formation of 8-hydroxy-2'-deoxyguanosine in DNA and induction of apoptotic cell death. Toxicol In Vitro. 2004;18:783-9.
81. Yu Z, Zhang L, Wu D, Liu F. Anti-apoptotic action of zearalenone in MCF-7 cells. Ecotoxicol Environ Saf. 2005;62:441-6.
82. Yu ZL, Zhang LS, Wu DS. Effects of zearalenone on proliferation and apoptosis in MCF-7 cells. Zhonghua Yu Fang Yi Xue Za Zhi. 2005;39:328-31.
83. Torkin R, Lavoie JF, Kaplan DR, Yeger H. Induction of caspase-dependent, p53-mediated apoptosis by apigenin in human neuroblastoma. Mol Cancer Ther. 2005 4:1-11.
84. Zheng PW, Chiang LC, Lin CC. Apigenin induced apoptosis through p53-dependent pathway in human cervical carcinoma cells. Life Sci. 2005;76:1367-79.
85. Roucou X, Montessuit S, Antonsson B, Martinou JC. Bax oligomerization in mitochondrial membranes requires tBid (caspase-8-cleaved Bid) and a mitochondrial protein. Biochem J. 2002;368:915-21.

86. Scorrano L, Korsmeyer SJ. Mechanisms of cytochrome c release by proapoptotic BCL-2 family members. Biochem Biophys Res Commun. 2003;304:437-44.
87. Korsmeyer SJ, Wei MC, Saito M, Weiler S, Oh KJ, Schlesinger PH. Pro-apoptotic cascade activates BID, which oligomerizes BAK or BAX into pores that result in the release of cytochrome c. Cell Death Differ. 2000;7:1166-73.
88. Svasti J, Srisomsap C, Subhasitanont P, Keeratichamroen S, Chokchaichamnankit D, Ngiwsara L, et al. Proteomic profiling of cholangiocarcinoma cell line treated with pomiferin from Derris malaccensis. Proteomics. 2005;5:4504-9.
89. Hara MR, Agrawal N, Kim SF, Cascio MB, Fujimuro M, Ozeki Y, et al. S-nitrosylated GAPDH initiates apoptotic cell death by nuclear translocation following Siah1 binding. Nat Cell Biol. 2005;7:665-74.
90. Xu C, Bailly-Maitre B, Reed JC. Endoplasmic reticulum stress: cell life and death decision. J Clin Invest. 2005;115:2656-64.
91. Zhang D, Armstrong JS. Bax and the mitochondrial permeability transition cooperate in the release of cytochrome c during endoplasmic reticulum-stress-induced apoptosis. Cell Death Differ. 2007;14:703-15.
92. Tufi R, Panaretakis T, Bianchi K, Criollo A, Fazi B, Di Sano F, et al. Reduction of endoplasmic reticulum calcium ion levels favors plasma membrane surface exposure of calreticulin. Cell Death Differ. 2007;14:1-9.
93. Lacour S, Micheau O, Hammann A, Drouineaud V, Tschopp J, Solary E, et al. Chemotherapy enhances TNF-related apoptosis-inducing ligand DISC assembly in HT29 human colon cancer cells. Oncogene. 2003;22:1807-16.
94. Luo X, Budihardjo I, Zou H, Slaughter C, Wang X. Bid, a Bcl2 interacting protein, mediates cytochrome c release from mitochondria in response to activation of cell surface death receptors. Cell. 1998;94:481-90.
95. Hengartner MO. The biochemistry of apoptosis. Nature. 2000;407:770-6.
96. Peng CH, Huang CN, Hsu SP, Wang CJ. Penta-acetyl geniposide-induced apoptosis involving transcription of NGF/p75 via MAPK-mediated AP-1 activation in C6 glioma cells. Toxicology. 2007;238:130-9.